

All order effective action for charge diffusion from Schwinger-Keldysh holography

Yanyan Bu^{*}

School of Physics, Harbin Institute of Technology, Harbin 150001, China

Tuna Demircik[†]

Asia Pacific Center for Theoretical Physics, Pohang, 37673, Korea

Michael Lublinsky[‡]

Department of Physics, Ben-Gurion University of the Negev, Beer-Sheva 84105, Israel

(Dated: December 22, 2024)

Abstract

An effective action for diffusion of a conserved $U(1)$ charge is derived to all orders in the derivative expansion within a holographic model dual to the Schwinger-Keldysh closed time path. A systematic approach to solution of the 5D Maxwell equations in a doubled Schwarzschild-AdS₅ black brane geometry is developed. Constitutive relation for the stochastic charge current is shown to have a term induced by thermal fluctuations (coloured noise). All transport coefficient functions parameterising the effective action and constitutive relations are computed analytically in the hydrodynamic expansion, and then numerically for finite momenta.

^{*} yybu@hit.edu.cn

[†] tuna.demircik@apctp.org

[‡] lublinm@bgu.ac.il

CONTENTS

1. Introduction	3
2. Effective field theory for charge diffusion	7
A. Effective action	8
B. Discrete symmetries	9
C. $U(1)$ current with thermal noise	10
3. Holographic setup	12
A. The geometry	12
B. Maxwell field in the bulk	13
C. Boundary effective action	15
4. Bulk dynamics: solutions and analysis	17
A. Discrete symmetries	17
B. Horizon matching conditions	20
C. Linearly independent solutions	21
D. Solutions over the entire radial contour: gluing at the horizon	25
E. From the bulk solutions to the effective action	28
5. Results for the TCFs	31
A. Analytical results	32
B. Numerical results at finite ω and q	38
The noise-noise correlator	40
6. Summary and Outlook	41
A. The effective action from the basis decomposition	44
B. Validating (4.16)	46
C. Son-Starinets prescription for retarded correlators revisited	47
D. Numerical results for w_5, w_7, w_8, w_9	51

Acknowledgements	51
References	52

1. INTRODUCTION

Hydrodynamics [1–3] is an effective long-time long-distance description of many-body systems at nonzero temperature. Within the hydrodynamic approximation, the entire dynamics of a microscopic theory is reduced to that of conserved macroscopic currents, such as expectation values of energy-momentum tensor or charge current operators computed in a locally near equilibrium thermal state. An essential element of any hydrodynamics is a constitutive relation which relates the macroscopic currents to fluid-dynamic variables (fluid velocity, conserved charge densities, etc), and to external forces. Derivative expansion in the fluid-dynamic variables accounts for deviations from thermal equilibrium. At each order, the derivative expansion is fixed by thermodynamics and symmetries, up to a finite number of transport coefficients (TCs) such as viscosity and diffusion coefficients. The latter are not calculable from hydrodynamics itself, but have to be determined from underlying microscopic theory or extracted from experiments. In general, relativistic hydrodynamics truncated to any fixed order has a well-known major conceptual problem—it violates causality. To restore causality one has to introduce higher order gradient terms. Generically, causality is restored only after all (infinite) order gradients are resummed, in a way providing a UV completion of the “old” hydrodynamics. A compact way of organising the resummation is by introducing, instead of order by order transport coefficients, *momenta-dependent transport coefficient functions* (TCFs) [4].

The focus of the present paper will be on $U(1)$ charge diffusion. The all order constitutive relation for the spatial current density J^i has the following general form

$$J^i = -\mathcal{D}\partial_i J^v + \sigma_e \mathcal{F}_{iv} + \sigma_m \partial_k \mathcal{F}_{ik}, \quad (1.1)$$

where J^v is the charge density, and \mathcal{F} is field strength of external $U(1)$ field \mathcal{A}_μ . The coefficients \mathcal{D} , σ_e , and σ_m are generalised diffusion constant, electric and magnetic conductivities. These coefficients are not constants but rather TCFs, that is, they are functions of four-momentum in Fourier space or functionals of space-time derivatives in the real space:

$$\mathcal{D}[\partial_v, \vec{\partial}^2] \rightarrow \mathcal{D}[\omega, q^2], \quad \sigma_e[\partial_v, \vec{\partial}^2] \rightarrow \sigma_e[\omega, q^2], \quad \sigma_m[\partial_v, \vec{\partial}^2] \rightarrow \sigma_m[\omega, q^2]. \quad (1.2)$$

Generically, (1.1) is a non-local constitutive relation expressible in terms of *memory functions*, the inverse Fourier transforms of the TCFs [5].

AdS/CFT correspondence [6–8] is the only known framework, which provides a tractable approach to strongly coupled regime of non-Abelian gauge theories at finite temperature and opens a possibility to explore their transport properties exactly, at least for a class of gauge theories for which gravity duals can be constructed. The holographic duality maps hydrodynamic fluctuations of a boundary fluid into gravitational perturbations of a stationary black brane in an asymptotic AdS space [9–14]. The original papers on the subject focused on shear viscosity over entropy density ratio and two-point retarded correlators. For the latter, Son and Starinets proposed a computational prescription [13, 15], to be discussed below. Since then, the field has developed in different directions. Second and higher order TCs were computed for various bulk models, while our team has focused on development of *all order resummation* technique [5, 16, 17]. Particularly, in [18] we used the Maxwell theory probing the Schwarzschild-AdS₅ background to compute the TCFs introduced in (1.1) and (1.2).

Classical hydrodynamics is dissipative with the TCs, or more generally TCFs, parameterising the rate of dissipation in the fluids. Yet, dissipation in non-equilibrium dynamics is tightly related to thermal fluctuations via fluctuation-dissipation relations (FDRs). The latter originate from the energy momentum conservation in a closed system, which includes an open subsystem and a thermal bath. A canonical example is Brownian motion of a particle in a thermal bath. FDR renders the diffusive motion of the particle into a stochastic process described by Langevin equation. Similarly, proper account of thermal fluctuations in fluids, and particularly in relativistic fluids, should render classical hydrodynamics into stochastic one. These ideas have sparked many interesting developments in formulating an effective field theory (EFT) approach to dissipative hydrodynamics [19–36], from which constitutive relations for the currents could be straightforwardly derived. In presence of fluctuations the conserved current is expected to take the form¹

$$J_i = -\mathcal{D}\partial_i J^v + \sigma_e \mathcal{F}_{iv} + \sigma_m \partial_k \mathcal{F}_{ik} + J_i^{\text{noise}}. \quad (1.3)$$

Here J_i^{noise} is a noise term representing thermal force.

¹ Strictly speaking, the constitutive relation (1.3) holds for quadratic EFTs only. Beyond that, the constitutive relation is non-linear.

There is also a phenomenological interest in fluctuating hydrodynamics, largely driven by studies of quark gluon plasma (QGP), for which relativistic hydrodynamics is instrumental. Phenomenological implications of fluctuating hydrodynamics for realistic systems such as QGP have been discussed in, e.g., [37–43]. Particularly, in a model independent way, thermal fluctuations can be integrated out, resulting in emergence of “effective” TCs and shifts in positions of the hydrodynamic poles. This idea was first considered in [37, 38, 44] and recently revisited within an EFT framework in [41]. While in most phenomenological applications the noise is assumed to be white, it is generically non-Gaussian and momenta dependent (coloured), see e.g [45, 46]. The discussion in [46] was based on an Israel-Stewart-type model for causal diffusion. The goal of the present paper is to put the above mentioned ideas into a more firm ground by learning about the noise structure to all orders in the gradient expansion from a holographic model, in which such questions can be addressed via a first principle calculation.

While traditional holographic approach based on black hole in AdS (BH-AdS) captures dissipative effects of the boundary dynamics, it does not include any fluctuation. In finite temperature QFT, the unified framework that includes both the fluctuation and dissipation is a closed time path (CTP) integral, also referred to as Schwinger-Keldysh (SK) formalism [47–49]. From the holographic perspective, a dual geometry must have SK contour at its conformal boundary [35, 36, 50–62]. In contrast to the single BH-AdS geometry, this is achieved via patching two Lorentzian BH-AdS geometries with an Euclidean BH-AdS geometry. Proper matching conditions for the bulk fields should be imposed at time-like surfaces at which the geometries are glued [51, 52, 58, 63].

An alternative prescription has been proposed in [59], in which, instead of gluing geometries, the radial (holographic) coordinate has been complexified and analytically continued around the event horizon, forming a geometry with two copies of BH-AdS space. This latter approach will be referred to as SK holography. Over the last couple of years, the SK holography was applied to open quantum systems. The questions about non-Gaussian noise and KMS relations for fermionic degrees of freedom were addressed in [64–68]. However, the open systems considered in [64–68] do not involve hydrodynamical low energy degrees of freedom, for which an EFT formalism to be discussed below is required.

After this general introduction, we briefly review our setup. We are going to study the $U(1)$ charge diffusion in a thermal plasma in 4d. This will be derived from a probe Maxwell

theory in the doubled Schwarzschild-AdS₅ geometry. For the holographic SK formalism we will closely follow [59], which derived an effective action for diffusion, up to second order in the derivative expansion. One of our results will be the effective action computed to all orders in the derivative expansion. We will demonstrate that, thanks to linearity of the Maxwell equations in the bulk, the resulting effective action is quadratic in the dynamical fields and takes the precise form proposed in [29] (see (2.1)). The latter was derived from general symmetry-based considerations. In the next section we will flash the relevant results from [29]. The core of our calculation is in solving the bulk equations of motion (EOMs) in the doubled Schwarzschild-AdS₅. Following the idea introduced by two of us in [16, 17], we will be solving the dynamical equations only, leaving the constraint aside. This makes it possible to construct the “*off-shell*” *constitutive relations* and “*off-shell*” *hydrodynamic effective action*. This approach is nowadays referred to as “off-shell” holography [35, 36]. At a technical level, our treatment of the bulk EOMs will be somewhat different and more systematic compared to that of [59]: we will first search for a complete set of independent solutions in a single copy of the doubled Schwarzschild-AdS₅, and then will carefully match the two segments of the doubled Schwarzschild-AdS₅ near the event horizon. In this respect our formalism is more in spirit of [51, 52]. The latter, however, glued geometries along the time-like surfaces. When expanded to second order in the derivatives, our results could be compared with those of [58, 59]. While most of the coefficients are found to match, there are also some disagreements between all three results. The comparison and discussion are presented in subsection 5 A.

The main results of this paper are

- Derivation from the SK holography of the effective action [29] for the charge diffusion, from which the constitutive relation with the noise term in the form (1.3) follows straightforwardly.
- Computation of all the TCFs parameterising the effective action. These are computed analytically up to the second order in the derivative expansion and then numerically for finite (large) momenta. All the TCFs are analytically shown to satisfy the symmetry-imposed relations introduced in [29].
- The noise-noise correlator is computed, showing non-locality in the space-time.
- Derivation of the prescription [13] for retarded two-point correlators, starting from the SK holography, as opposed to the original work based on a single BH-AdS geometry (see Appendix C).

The paper is structured as follows. In Section 2, the effective action [29] for the diffusion at quadratic order and the TCFs parameterising it are reviewed. This Section also introduces the symmetry-induced relations among the TCFs and a discussion of the constitutive relations for the current with noise. The SK holography is introduced in Section 3. Solutions to the Maxwell's equation in the bulk are presented in Section 4. The results for the TCFs as well as noise-noise correlator are presented in Section 5. A brief summary and outlook is presented in Section 6. The effective action for the charge diffusion proposed in [29] is derived in Appendix A. A subtle point regarding the near-horizon matching condition for the time component of the bulk gauge field is further clarified in Appendix B. In Appendix C, the prescription [13] for retarded current-current correlators is derived starting from the SK holography. In Appendix D, the numerical results for independent TCFs (say, $w_{5,7,8,9}$) parameterising the effective action are presented.

Note added: While preparing this paper for release, we got aware of the recent work [69]. Just like us, [69] considers the Maxwell's theory within the SK holography and constructs an EFT for stochastic diffusion. Both papers employ the time-reversal symmetry to relate the ingoing modes (dissipation) with the outgoing modes (fluctuation/Hawking radiation). Our first impression is that [69] constructed EFT on-shell only, whereas we have obtained results for both on-shell and off-shell EFTs. Particularly, if our understanding is correct, Chapter 8 of [69] is quite similar to our Appendix C. Admittedly, a much more careful study of [69] would be needed to fully appreciate the degree of overlap and agreement between the two papers.

2. EFFECTIVE FIELD THEORY FOR CHARGE DIFFUSION

In this section, we review the hydrodynamic effective action derived in [29] and the symmetry properties of the TCFs parameterising it. We will also address the constitutive relation for the fluctuating $U(1)$ current. Finally, we present the general structure of the momenta-dependent (coloured) noise and the noise-noise correlator.

A. Effective action

At quadratic level in the dynamical fields, the most general form of the effective action for the $U(1)$ charge diffusion was derived in [29]:

$$S_{\text{eff}} = \int d^4x \mathcal{L}_{\text{eff}}(x), \quad (2.1)$$

where the effective Lagrangian is

$$\begin{aligned} \mathcal{L}_{\text{eff}} = & \frac{i}{2} B_{av}(x) w_1 B_{av}(x) + \frac{i}{2} B_{ak}(x) w_2 B_{ak}(x) + \frac{i}{2} \partial_k B_{ak}(x) w_3 \partial_l B_{al}(x) \\ & + i B_{av}(x) w_4 \partial_k B_{ak}(x) + B_{av}(x) w_5 B_{rv}(x) + B_{av}(x) w_6 \partial_v \partial_k B_{rk}(x) \\ & + \partial_k B_{ak}(x) w_7 B_{rv}(x) + B_{ak}(x) w_8 \partial_v B_{rk}(x) + \frac{1}{2} \mathcal{F}_{akl}(x) w_9 \mathcal{F}_{rkl}(x), \end{aligned} \quad (2.2)$$

where

$$B_{r\mu} = \frac{1}{2}(B_{1\mu} + B_{2\mu}), \quad B_{a\mu} = B_{1\mu} - B_{2\mu}. \quad (2.3)$$

In (2.2), $\mathcal{F}_{r\mu\nu}$ and $\mathcal{F}_{a\mu\nu}$ are the field strengths of $B_{r\mu}$ and $B_{a\mu}$, respectively. Here, $B_{1\mu}$ and $B_{2\mu}$ live on the upper and lower branches of the SK contour, and are defined as independent $U(1)$ gauge transforms of the background gauge fields $\mathcal{A}_{1\mu}$ and $\mathcal{A}_{2\mu}$ [29]

$$B_{1\mu} \equiv \mathcal{A}_{1\mu} + \partial_\mu \varphi_1, \quad B_{2\mu} \equiv \mathcal{A}_{2\mu} + \partial_\mu \varphi_2, \quad (2.4)$$

where the gauge transformation parameters φ_1 and φ_2 are treated as low energy hydrodynamical modes.

The parameters $w_{1\dots 9}$ are the TCFs: they are $SO(3)$ scalar functionals of the space-time derivatives. As explained in section 1, in momentum space these TCFs become functions of frequency ω and spatial momentum \vec{q} .

The generating functional $W[\mathcal{A}_{a\mu}, \mathcal{A}_{r\mu}]$ is obtained by integrating over the dynamical fields φ_1 and φ_2 or, alternatively, over φ_r and φ_a :

$$e^{W[\mathcal{A}_{a\mu}, \mathcal{A}_{r\mu}]} \equiv \int D\varphi_r D\varphi_a e^{iS_{\text{eff}}[B_{a\mu}, B_{r\mu}]}. \quad (2.5)$$

Normalisation of W is such that $W[\mathcal{A}_{a\mu} = 0, \mathcal{A}_{r\mu}] = 0$.

The hydrodynamic effective action (2.1) could be thought of as being obtained by integrating out the gapped modes of an underlying microscopic theory defined on the CTP (SK

contour). While the microscopic theory is formulated on the SK contour, the low energy EFT (2.1) (also (2.5)) is defined with time running forward only, along the real axes.

Two currents defined as

$$J_r^\mu(x) = \frac{\delta S_{\text{eff}}}{\delta \mathcal{A}_{a\mu}(x)}, \quad J_a^\mu(x) = \frac{\delta S_{\text{eff}}}{\delta \mathcal{A}_{r\mu}(x)} \quad (2.6)$$

are conserved by the EOMs for the dynamical fields φ_r and φ_a , which are derived from variation of the effective action (2.1).

B. Discrete symmetries

The effective action S_{eff} possesses several discrete symmetries, including parity \mathcal{P} and time reversal \mathcal{T} , inherited from the underlying microscopic theory. These symmetries impose relations among the TCFs w_i 's, which we review here, see [29] for details.

- Z_2 -reflection symmetry:

$$S_{\text{eff}}[B_{1\mu}; B_{2\mu}] = -S_{\text{eff}}[B_{2\mu}; B_{1\mu}], \quad (2.7)$$

which implies that the coefficients of the leading terms in the derivative expansion of w_i 's must be non-negative.

- \mathcal{T} -symmetry of (2.2) translates into local KMS conditions,

$$w_1 = -\frac{i}{2} \coth \frac{\beta\omega}{2} (w_5 - w_5^*), \quad (2.8)$$

$$w_2 + w_3 q^2 = -\frac{\omega}{2} \coth \frac{\beta\omega}{2} (w_8 + w_8^*), \quad w_3 = \frac{i}{2} \coth \frac{\beta\omega}{2} (w_9 - w_9^*), \quad (2.9)$$

$$w_4 = -\frac{1}{2} \coth \frac{\beta\omega}{2} (\omega w_6 - i w_7^*). \quad (2.10)$$

- \mathcal{PT} -symmetry leads to Onsager relations,

$$w_4 = -w_4^*, \quad \omega w_6 = -i w_7, \quad (2.11)$$

which makes it possible to rewrite the relation (2.10) as

$$w_4 = \frac{i}{2} \coth \frac{\beta\omega}{2} (w_7 + w_7^*) = -\frac{\omega}{2} \coth \frac{\beta\omega}{2} (w_6 - w_6^*). \quad (2.12)$$

The TCFs w_1, w_2, w_3 are real functions of ω and q , while w_4 is purely imaginary. Overall, there are *four* independent parameters in (2.2), which could be taken as w_5, w_7 (or

equivalently w_6), w_8 and w_9 . The non-fluctuating $U(1)$ current has three TCFs only (see (2.16)). Yet, stochastic $U(1)$ current possesses an additional TCF. While the effective action/constitutive relations are parameterised by four (independent) coefficients, the number of independent two-point correlators is only two, with the others being related by the FDR.

The main goal of the present paper is to derive (2.2) from a holographic model and compute w_i 's to all orders in the derivative expansion. It will be demonstrated analytically that all the symmetry induced relations introduced above are automatically satisfied by the holographic construction.

C. $U(1)$ current with thermal noise

From (2.6) (see also equations (4.21)-(4.23) in [29]),

$$\begin{aligned} J_r^v &= w_5 B_{rv} + w_6 \partial_v \partial_k B_{rk} + i w_1 B_{av} + i w_4 \partial_k B_{ak} \\ J_r^i &= -w_7 \partial_i B_{rv} + w_8 \partial_v B_{ri} + w_9 \partial_k \mathcal{F}_{rik} + i w_2 B_{ai} - i w_3 \partial_i \partial_l B_{al} - i w_4^* \partial_i B_{av} \\ J_a^v &= w_5^* B_{av} + w_7^* \partial_k B_{ak} \\ J_a^i &= w_6^* \partial_v \partial_i B_{av} - w_8^* \partial_v B_{ai} + w_9^* \partial_k \mathcal{F}_{aik} \end{aligned} \quad (2.13)$$

When $B_a = 0$, J_a^μ vanishes while J_r^μ becomes the hydrodynamic current J_{hydro}^μ [29]:

$$\begin{aligned} J_{hydro}^v &= w_5 B_{rv} + w_6 \partial_v \partial_k B_{rk} = (w_5 + w_6 \vec{\partial}^2) \mu - w_6 \partial_k \mathcal{F}_{rk v}, \\ J_{hydro}^i &= -w_7 \partial_i B_{rv} + w_8 \partial_v B_{ri} + w_9 \partial_k \mathcal{F}_{rik} = (w_8 - w_7) \partial_i \mu - w_8 \mathcal{F}_{riv} + w_9 \partial_k \mathcal{F}_{rik} \end{aligned} \quad (2.14)$$

J_{hydro}^v is the charge density and $\mu = B_{rv}$ is identified with the chemical potential. With μ replaced by the charge density, the current density \vec{J}_{hydro} is cast into the same form (1.1) as that of [18]

$$J_{hydro}^i = -\mathcal{D} \partial_i J_{hydro}^v + \sigma_e \mathcal{F}_{riv} + \sigma_m \partial_k \mathcal{F}_{rik}, \quad (2.15)$$

where

$$\mathcal{D} = \frac{w_7 - w_8}{w_5 + w_6 \vec{\partial}^2}, \quad \sigma_e = \frac{w_8 - w_7}{w_5 + w_6 \vec{\partial}^2} w_6 \vec{\partial}^2 - w_8, \quad \sigma_m = w_9 - \frac{w_8 - w_7}{w_5 + w_6 \vec{\partial}^2} w_6 \partial_v. \quad (2.16)$$

Thermal fluctuations are turned on by relaxing $B_a = 0$ approximation. We can still set $\mathcal{A}_{1\mu} = \mathcal{A}_{2\mu} = \mathcal{A}_\mu$, since \mathcal{A}_μ is an external field, which is not necessarily assumed to be fluctuating:

$$B_{r\mu} = \mathcal{A}_\mu + \partial_\mu \varphi_r \quad B_{a\mu} = \partial_\mu \varphi_a \quad (2.17)$$

The φ_a field acts as a source of noise both for the charge density and hydrodynamic current \vec{J}_{hydro} :

$$\begin{aligned} J_r^v &= J_{hydro}^v + i(w_1\partial_v + w_4\vec{\partial}^2)\varphi_a, & J_r^i &= J_{hydro}^i + i(w_2 - w_3\vec{\partial}^2 - w_4^*\partial_v)\partial_i\varphi_a, \\ J_a^v &= (w_5^*\partial_v + w_7^*\vec{\partial}^2)\varphi_a, & J_a^i &= (w_6^*\partial_v^2\partial_i - w_8^*\partial_v\partial_i)\varphi_a \end{aligned} \quad (2.18)$$

The first line of (2.18) is an all order stochastic constitutive relation for the conserved current J_r^μ , which can be recast into

$$J_r^i = -\mathcal{D}\partial_i J_r^v + \sigma_e \mathcal{F}_{iv} + \sigma_m \partial_k \mathcal{F}_{ik} + \Xi \partial_i \varphi_a, \quad (2.19)$$

where the Ξ -term acts as a thermal force:

$$\Xi = i\mathcal{D}(w_1\partial_v + w_4\vec{\partial}^2) + i(w_2 - w_3\vec{\partial}^2 - w_4^*\partial_v) \quad (2.20)$$

While J_r^μ is conserved, in presence of thermal fluctuations, the hydrodynamical current J_{hydro}^μ is not:

$$\partial_\mu J_{hydro}^\mu = \xi, \quad \xi \equiv G_0 \varphi_a \quad (2.21)$$

with

$$\begin{aligned} G_0 &= -i \left[w_1\partial_v^2 + w_4\partial_v\vec{\partial}^2 + (w_2 - w_3\vec{\partial}^2)\vec{\partial}^2 - w_4^*\partial_v\vec{\partial}^2 \right] \\ &= i \coth \frac{\beta\omega}{2} \left\{ \omega^2 \text{Im}(w_5) - \omega q^2 \text{Re}(w_8) + 2\omega q^2 \text{Re}(w_7) \right\} \\ &= i \coth \frac{\beta\omega}{2} \left\{ \omega^2 \text{Im}(w_5) - \omega q^2 \text{Re}(w_8) - 2\omega^2 q^2 \text{Im}(w_6) \right\} \end{aligned} \quad (2.22)$$

G_0 is clearly purely imaginary. We have recast the continuity equation into the usual stochastic form. Worth noticing that the noise is a scalar, that is only the longitudinal sector is fluctuating. This reflects the fact that physically the quantity that actually fluctuates is the charge density. There are no fluctuations in the transverse sector, in which the current is induced by the external fields, assuming the latter are not fluctuating.

The noise is Gaussian but coloured as it depends on four-momentum. Changing variable from φ_a to ξ in the action S_{eff} results in the following noise-noise correlator

$$\langle \xi(x) \xi(0) \rangle = \tilde{G}_0(x) \quad (2.23)$$

where $\tilde{G}_0(x)$ is the inverse Fourier transformation of $-iG_0$. Since $-iG_0$ is a real function in the momentum space, the noise-noise correlator is symmetric as expected. Numerical results for \tilde{G}_0 will be presented in subsection 5B. Contrary to the white noise behaviour (δ -functional form for \tilde{G}_0) we will observe non-local space-time effects in the noise sector.

3. HOLOGRAPHIC SETUP

A. The geometry

The metric of Schwarzschild-AdS₅ in the ingoing Eddington-Finkelstein (EF) coordinate system $x^M = (r, v, x^i)$ is given by the line element

$$ds^2 = g_{MN}dx^M dx^N = -f(r)dv^2 + 2dvdr + r^2\delta_{ij}dx^i dx^j, \quad i, j = 1, 2, 3, \quad (3.1)$$

where $f(r) = r^2 - r_h^4/r^2$. We will also use the Schwarzschild coordinate system $\tilde{x}^M = (r, t, x^i)$, for which the metric (3.1) is

$$ds^2 = \tilde{g}_{MN}d\tilde{x}^M d\tilde{x}^N = \frac{dr^2}{f(r)} - f(r)dt^2 + r^2\delta_{ij}dx^i dx^j, \quad i, j = 1, 2, 3. \quad (3.2)$$

In both (3.1) and (3.2), the curvature radius of the AdS space is set to unity.

The holographic geometry dual to thermal state with the SK contour at the boundary is a doubled Schwarzschild-AdS₅. We will closely follow the holographic prescription of [59], which doubled the geometry (3.1) by complexifying the radial coordinate r along the contour illustrated in Figure 1.

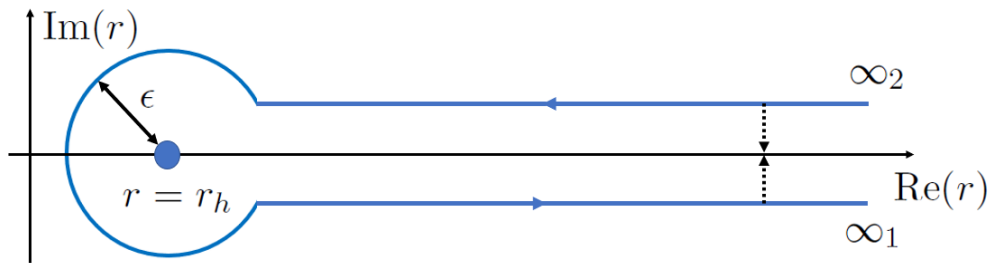


FIG. 1: The holographic SK contour of [59]: the complexified radial coordinate analytically continued around the event horizon $r = r_h$. The dashed arrows indicate that the horizontal segments are infinitesimally close to the real axis.

The two ends of the r contour are identified with the SK contour of the boundary theory [48, 49], the infinitesimally small horizon circle is mapped into initial thermal state, while the horizontal segments reflect the CTP. The holographic contour 1 is obtained by taking two exteriors of an eternal AdS₅ black hole [70] and identifying their future horizons.

The EF time v is related to the Schwarzschild time t by

$$t = v - \zeta_2(r), \quad \zeta_2(r) \equiv \int_{\infty_2}^r \frac{dy}{f(y)}, \quad r \in [r_h - \epsilon, \infty_2),$$

$$t = v - \zeta_1(r), \quad \zeta_1(r) \equiv \int_{\infty_1}^r \frac{dy}{f(y)}, \quad r \in [r_h - \epsilon, \infty_1), \quad (3.3)$$

where the integration constants are fixed by requirement that t and v coincide on the AdS boundaries. An interesting observation is that viewed in the ingoing EF coordinate (that is the EF time v is identical everywhere along the radial contour), the Schwarzschild time t is discontinuous at $r = r_h - \epsilon$,

$$t^{\text{up}}(r_h - \epsilon) - t^{\text{dw}}(r_h - \epsilon) = \int_{\infty_1}^{\infty_2} \frac{dy}{f(y)} = -\frac{i\pi}{2r_h} = -\frac{i\beta}{2}, \quad (3.4)$$

where β is inverse of the black brane temperature T . This becomes important when gluing bulk fields of the upper and lower segments of the contour in Figure 1.

B. Maxwell field in the bulk

The holographic model for the $U(1)$ diffusion is a probe Maxwell field in the above described geometry. The bulk action is

$$S_0 = -\frac{1}{4} \int d^4x \int_{\infty_2}^{\infty_1} dr \sqrt{-g} F_{MN} F^{MN} \quad (3.5)$$

$$= -\frac{1}{4} \int d^4\tilde{x} \int_{\infty_2}^{\infty_1} dr \sqrt{-\tilde{g}} \tilde{F}_{MN} \tilde{F}^{MN}, \quad (3.6)$$

where C_N and \tilde{C}_N are the $U(1)$ bulk gauge fields in EF and Schwarzschild coordinate systems respectively; $F_{MN} = \nabla_M C_N - \nabla_N C_M$ and $\tilde{F}_{MN} = \tilde{\nabla}_M \tilde{C}_N - \tilde{\nabla}_N \tilde{C}_M$. To remove the UV divergences near the AdS boundaries $r = \infty_1$ and $r = \infty_2$, the bulk action (3.5) (or (3.6)) should be supplemented with a counter-term action:

$$S_{\text{c.t.}} = \frac{1}{4} \log r \int d^4x \sqrt{-\gamma} F_{\mu\nu} F^{\mu\nu} \Big|_{r=\infty_1} - \frac{1}{4} \log r \int d^4x \sqrt{-\gamma} F_{\mu\nu} F^{\mu\nu} \Big|_{r=\infty_2}, \quad (3.7)$$

where the indices are contracted with the induced metric $\gamma_{\mu\nu}$

$$ds^2|_{\Sigma} = \gamma_{\mu\nu} dx^\mu dx^\nu = -f(r) dv^2 + r^2 \delta_{ij} dx^i dx^j. \quad (3.8)$$

Here Σ denotes either the hypersurface $r = \infty_1$ or $r = \infty_2$. The counter-term action in the Schwarzschild coordinate system is the same as (3.7), since $v = t$ at the AdS boundaries. The minimal subtraction scheme (3.7) differs from that used in [59].

Transformation rule for the fields from the EF coordinate system to the Schwarzschild can be easily derived from the coordinate-invariants

$$\tilde{C}_M d\tilde{x}^M = C_M dx^M, \quad (3.9)$$

leading to

$$\tilde{C}_t(r, t, \vec{x}) = C_v(r, v, \vec{x}), \quad \tilde{C}_i(r, t, \vec{x}) = C_i(r, v, \vec{x}). \quad (3.10)$$

The radial components of the bulk gauge field differ

$$\tilde{C}_r(r, t, \vec{x}) - \frac{\tilde{C}_t(r, t, \vec{x})}{f(r)} = C_r(r, v, \vec{x}) \implies \tilde{C}_r(r, t, \vec{x}) = C_r(r, v, \vec{x}) + \frac{C_v(r, v, \vec{x})}{f(r)}. \quad (3.11)$$

Thus it is important to distinguish between two radial gauge choices:

$$\begin{aligned} \text{Schwarzschild radial gauge :} \quad \tilde{C}_r = 0 &\iff C_r = -\frac{C_v}{f(r)}, \\ \text{EF radial gauge :} \quad C_r = 0 &\iff \tilde{C}_r = \frac{\tilde{C}_t}{f(r)}. \end{aligned} \quad (3.12)$$

The EF radial gauge is most commonly used, including in [59]. Yet, for reasons related to time-reversal symmetry which will be explained in the next section, we chose to perform calculations in the Schwarzschild radial gauge.

Bulk EOMs are derived by variation of (3.5) and (3.6):

$$\nabla_M F^{MN} = 0 \implies \frac{1}{\sqrt{-g}} \partial_M (\sqrt{-g} F^{MN}) = 0, \quad (3.13)$$

$$\tilde{\nabla}_M \tilde{F}^{MN} = 0 \implies \frac{1}{\sqrt{-\tilde{g}}} \tilde{\partial}_M (\sqrt{-\tilde{g}} \tilde{F}^{MN}) = 0. \quad (3.14)$$

With the help of (3.10) and (3.11), the two sets of the Maxwell equations can be related

$$\tilde{\nabla}_M \tilde{F}^{Mr} = \nabla_M F^{Mr}, \quad \tilde{\nabla}_M \tilde{F}^{Mt} = \nabla_M F^{Mv} - \frac{1}{f(r)} \nabla_M F^{Mr}, \quad \tilde{\nabla}_M \tilde{F}^{Mi} = \nabla_M F^{Mi}. \quad (3.15)$$

The first equation (the r -component) is a gauge invariant constraint, which will play a special role in our construction. When all the bulk equations are solved (i.e., on-shell holography), (3.13) and (3.14) are absolutely equivalent as is obvious from (3.15). Yet, in [18] we argued that in order to compute the TCFs parameterising the (off-shell) constitutive relations for the current, it is sufficient to solve the bulk dynamical equations only, while leaving the constraint aside. Within the holographic prescription the constraint is mapped into continuity equation for the current at the boundary, which is the dynamical equation for the low energy modes φ_1 and φ_2 . Derivation of the effective action follows the very same strategy as introduced in [5, 16–18], now frequently referred to as off-shell holography [35, 36].

We are going to solve the EOMs in the Schwarzschild coordinates and then re-express the results in the EF coordinates using (3.10) and (3.11). In the spirit of the off-shell formalism, we will not impose the constraint equation. Hence, the dynamical equations which will be solved are

$$\nabla_M F^{Mv} - \frac{1}{f(r)} \nabla_M F^{Mr} = 0 \iff \tilde{\nabla}_M \tilde{F}^{Mt} = 0, \quad \nabla_M F^{Mi} = 0 \iff \tilde{\nabla}_M \tilde{F}^{Mi} = 0. \quad (3.16)$$

Notice that the first equation differs from $\nabla_M F^{Mv} = 0$ derived in the EF coordinates. The seemingly freedom to modify the dynamical equation is eliminated when the Schwarzschild radial gauge is implemented in the effective action.

The dynamical equations (3.16) are instrumental in deriving a holographic RG flow-like equation for $\nabla_M F^{Mr}$:

$$\partial_r (\sqrt{-g} \nabla_M F^{Mr}) = \frac{i\omega}{f(r)} \sqrt{-g} \nabla_M F^{Mr}, \quad (3.17)$$

which is solved by

$$\begin{aligned} \sqrt{-g} \nabla_M F^{Mr} &= \mathcal{C}^{\text{up}}(k) e^{i\omega\zeta_2(r)}, & r \in [r_h - \epsilon, \infty_2), \\ \sqrt{-g} \nabla_M F^{Mr} &= \mathcal{C}^{\text{dw}}(k) e^{i\omega\zeta_1(r)}, & r \in [r_h - \epsilon, \infty_1). \end{aligned} \quad (3.18)$$

Here, $\mathcal{C}^{\text{up}, \text{dw}}$ are r -independent integration constants in either upper or lower segments of the r -contour. Both vanish on-shell.

C. Boundary effective action

Integrating by parts, the bulk action (3.5) can be expressed as

$$\begin{aligned} S_0 &= -\frac{1}{2} \int d^4x \int_{\infty_2}^{\infty_1} dr \sqrt{-g} [\nabla_M (C_N F^{MN}) - C_N \nabla_M F^{MN}] \\ &= \frac{1}{2} \int d^4x \int_{\infty_2}^{\infty_1} dr \sqrt{-g} [C_r \nabla_M F^{Mr} + C_v \nabla_M F^{Mv} + C_k \nabla_M F^{Mk}] \\ &\quad - \frac{1}{2} \int d^4x \sqrt{-\gamma} n_M C_N F^{MN} \Big|_{r=\infty_2}^{r=\infty_1} \\ &= \frac{1}{2} \int d^4x \int_{\infty_2}^{\infty_1} dr \sqrt{-g} \left\{ C_v \left[\nabla_M F^{Mv} - \frac{1}{f(r)} \nabla_M F^{Mr} \right] + C_k \nabla_M F^{Mk} \right. \\ &\quad \left. + \left(C_r + \frac{C_v}{f(r)} \right) \nabla_M F^{Mr} \right\} - \frac{1}{2} \int d^4x \sqrt{-\gamma} n_M C_N F^{MN} \Big|_{r=\infty_2}^{r=\infty_1}. \end{aligned} \quad (3.19)$$

Here n_M is a unit out-pointing normal vector to the hypersurface Σ . All the bulk terms in (3.19) vanish either thanks to the dynamical equations (3.16) or the Schwarzschild radial gauge². Eventually, the resulting action becomes a superposition of two surface terms

$$S_0 = -\frac{1}{2} \int d^4x \sqrt{-\gamma} n_M C_N F^{MN} \Big|_{r=\infty_2}^{r=\infty_1}. \quad (3.20)$$

There is a subtle point in deriving (3.20). As will become clear in the next section, in the off-shell formalism, the gauge potential and/or field strength develop discontinuity near the event horizon. Hence, in principle, there might emerge an additional boundary term at the horizon surface. This term will be eliminated by a specific choice of the boundary conditions to be discussed below.

The bulk EOMs (3.16) will be solved subject to boundary conditions at two AdS boundaries $r = \infty_1$ and $r = \infty_2$:

$$C_\mu \xrightarrow{r \rightarrow \infty_1} B_{1\mu}(x^\alpha) \equiv \mathcal{A}_{1\mu} + \partial_\mu \varphi_1, \quad C_\mu \xrightarrow{r \rightarrow \infty_2} B_{2\mu}(x^\alpha) \equiv \mathcal{A}_{2\mu} + \partial_\mu \varphi_2. \quad (3.21)$$

In order to compute the boundary action (3.20), near boundary asymptotic expansion of the bulk fields is required. It has the form

$$C_\mu \xrightarrow{r \rightarrow \infty_1} B_{1\mu}(x^\alpha) + \frac{\partial_\nu B_{1\mu}(x^\alpha)}{r} - \frac{1}{2} \partial^\nu \mathcal{F}_{1\mu\nu}(x^\alpha) \frac{\log r}{r^2} + \frac{C_{1\mu}^{(2)}(x^\alpha)}{r^2} + \dots, \quad (3.22)$$

$$C_\mu \xrightarrow{r \rightarrow \infty_2} B_{2\mu}(x^\alpha) + \frac{\partial_\nu B_{2\mu}(x^\alpha)}{r} - \frac{1}{2} \partial^\nu \mathcal{F}_{2\mu\nu}(x^\alpha) \frac{\log r}{r^2} + \frac{C_{2\mu}^{(2)}(x^\alpha)}{r^2} + \dots, \quad (3.23)$$

where the coefficient functions $C_{1\mu}^{(2)}$ and $C_{2\mu}^{(2)}$ are functionals both of $B_{1\mu}$ and $B_{2\mu}$. They will be determined through the solution of the dynamical equations (3.16) over the entire contour in Figure. 1. This is the subject of the next section.

Once (3.22) and (3.23) are substituted into the total action $S_{\text{eff}} = S_0 + S_{\text{c.t.}}$, the latter takes the form (2.1) with the effective Lagrangian $\mathcal{L}_{\text{eff}}(x)$ being a quadratic functional of the boundary fields $B_{1\mu}$ and $B_{2\mu}$ (in the (r, a) -basis)

$$\begin{aligned} \mathcal{L}_{\text{eff}} = & -B_{rv}(C_{1v}^{(2)} - C_{2v}^{(2)}) - \frac{1}{2} B_{av}(C_{1v}^{(2)} + C_{2v}^{(2)}) + B_{rk}(C_{1k}^{(2)} - C_{2k}^{(2)}) \\ & + \frac{1}{2} B_{ak}(C_{1k}^{(2)} + C_{2k}^{(2)}) + \frac{1}{2} \partial_k B_{ak} \partial_v B_{rv} - \frac{1}{2} B_{av} \partial_v \partial_k B_{rk} \\ & - \frac{1}{2} B_{ak} \partial_v^2 B_{rk} + \frac{1}{4} \mathcal{F}_{akj} \mathcal{F}_{rkj} + \frac{1}{2} B_{av} \vec{\partial}^2 B_{rv} + B_{av} \partial_v^2 B_{rv}. \end{aligned} \quad (3.24)$$

² In [59], the EF radial gauge $C_r = 0$ was taken, combined with the dynamical equations $\nabla_M F^{Mv} = 0$ and $\nabla_M F^{Mi} = 0$, which also eliminated the bulk terms in (3.19) leading to the very same boundary action.

With the help of a basis decomposition procedure introduced in [18], the effective Lagrangian (3.24) can be recast into the form (2.2), thus providing a holographic derivation of the latter, which is fully consistent with the general analysis of [29]. This derivation is presented in Appendix A.

4. BULK DYNAMICS: SOLUTIONS AND ANALYSIS

This section is devoted to solutions of the bulk EOMs (3.16) over the contour displayed in Figure 1. Our strategy will be different from that of [59]. Instead of integrating the bulk EOMs (3.16) along the entire r -contour, we split the radial contour at $r = r_h - \epsilon$ into two segments, the upper and lower one. Each segment “lives” in a single copy of the doubled Schwarzschild-AdS₅ geometry. In each segment, there is a set of independent solutions to the dynamical EOMs (3.16) forming a basis. Full solutions obeying the respective boundary conditions (3.21) will be constructed as linear superpositions of the basis solutions. Thus-constructed piecewise solutions will be carefully glued at the cutting slice $r = r_h - \epsilon$, under proper matching conditions to be derived in subsection 4B. One of the advantages of our approach is that it avoids the subtleties related to non-commutativity between two limits: the hydrodynamic derivative expansion and $\epsilon \rightarrow 0$, the latter has to be taken first.

A. Discrete symmetries

Symmetries in classical theories are used in order to generate solutions, if one is already known. Maxwell’s theory in the bulk (single copy Schwarzschild-AdS) has a number of discrete symmetries, such as parity and time reversal, which will be employed in our quest after a full set of independent solutions. However, in different coordinate systems, the symmetries are represented differently. Particularly, while in the Schwarzschild coordinates the time reversal symmetry is realised trivially, its representation in the EF coordinates is much less transparent. This is essentially the main reason we have chosen to first find all the solutions in the Schwarzschild coordinates and then translate those into the EF system.

In the Schwarzschild coordinates (without any gauge fixing yet), the Fourier mode $\tilde{C}_M(r, k^\mu)$ defined by

$$\tilde{C}_M(r, t, x^i) = \int \frac{d^4 k}{(2\pi)^4} e^{ik \cdot x} \tilde{C}_M(r, k^\mu), \quad (4.1)$$

satisfies the following system of ODEs:

$$\tilde{\nabla}_M \tilde{F}^{Mr} = 0 \Rightarrow 0 = (i\omega \partial_r \tilde{C}_t - \omega^2 \tilde{C}_r) + r^{-2} f(r) (q^2 \tilde{C}_r + iq_k \partial_r \tilde{C}_k), \quad (4.2)$$

$$\tilde{\nabla}_M \tilde{F}^{Mt} = 0 \Rightarrow 0 = \partial_r (r^3 \partial_r \tilde{C}_t) + i\omega \partial_r (r^3 \tilde{C}_r) - \frac{r}{f(r)} (q^2 \tilde{C}_t + \omega q_k \tilde{C}_k), \quad (4.3)$$

$$\begin{aligned} \tilde{\nabla}_M \tilde{F}^{Mi} = 0 \Rightarrow 0 = & \partial_r [r f(r) \partial_r \tilde{C}_i] - iq_i \partial_r [r f(r) \tilde{C}_r] + \frac{r}{f(r)} (\omega^2 \tilde{C}_i + \omega q_i \tilde{C}_t) \\ & + r^{-1} (-q^2 \tilde{C}_i + q_i q_k \tilde{C}_k). \end{aligned} \quad (4.4)$$

The full set of bulk EOMs (4.2)-(4.4) is obviously invariant under the following time-reversal transformation:

$$\begin{aligned} \omega &\rightarrow -\omega, & \tilde{C}_t(r, k^\mu) &\rightarrow \tilde{C}_t(r, \bar{k}^\mu), & \tilde{C}_i(r, k^\mu) &\rightarrow -\tilde{C}_i(r, \bar{k}^\mu), \\ \tilde{C}_r(r, k^\mu) &\rightarrow -\tilde{C}_r(r, \bar{k}^\mu), & \text{with } \bar{k}^\mu &= (-\omega, \vec{q}), \end{aligned} \quad (4.5)$$

which, in the coordinate space (r, t, \vec{x}) , turns into

$$\begin{aligned} t &\rightarrow -t, & \tilde{C}_t(r, t, \vec{x}) &\rightarrow \tilde{C}_t(r, -t, \vec{x}), & \tilde{C}_i(r, t, \vec{x}) &\rightarrow -\tilde{C}_i(r, -t, \vec{x}), \\ \tilde{C}_r(r, t, \vec{x}) &\rightarrow -\tilde{C}_r(r, -t, \vec{x}). \end{aligned} \quad (4.6)$$

Furthermore, the dynamical EOMs (4.3) and (4.4) are invariant under the time reversal independently, regardless of the constraint equation (4.2) being imposed or not. Transformations (4.5) and (4.6) can be recognised as a *linear* realisation of the time-reversal symmetry [64].

In the ingoing EF coordinates (3.1), the Fourier mode $C_M(r, k^\mu)$ defined by

$$C_M(r, x^\mu) = \int \frac{d^4 k}{(2\pi)^4} e^{ik \cdot x} C_M(r, k^\mu), \quad k^\mu = (\omega, \vec{q}), \quad (4.7)$$

obeys another system of ODEs:

$$\nabla_M F^{Mr} = 0 \Rightarrow 0 = r^3 (\omega^2 C_r - i\omega \partial_r C_v) - r f(r) (q^2 C_r + iq_k \partial_r C_k) - r (q^2 C_v + \omega q_k C_k), \quad (4.8)$$

$$\begin{aligned} \nabla_M F^{Mv} - \frac{1}{f(r)} \nabla_M F^{Mr} = 0 \Rightarrow 0 = & \partial_r (r^3 \partial_r C_v + i\omega r^3 C_r) + r (q^2 C_r + iq_k \partial_r C_k) \\ & + \frac{r^3}{f(r)} (\omega^2 C_r - i\omega \partial_r C_v) - \frac{r}{f(r)} (q^2 C_v + \omega q_k C_k) - r (q^2 C_r + iq_k \partial_r C_k), \end{aligned} \quad (4.9)$$

$$\begin{aligned} \nabla_M F^{Mi} = 0 \Rightarrow 0 = & \partial_r [r f(r) (\partial_r C_i - iq_i C_r)] - \partial_r [r (i\omega C_i + iq_i C_v)] \\ & - r (i\omega \partial_r C_i + \omega q_i C_r) + r^{-1} (-q^2 C_i + q_i q_k C_k). \end{aligned} \quad (4.10)$$

Apparently, the transformation like (4.5) is not a symmetry of EOMs (4.8)-(4.10). This is related to the fact that $v \rightarrow -v$ is not a symmetry, because the transformation does not leave the metric (3.1) invariant. This point was made clear in [64], which carried a somewhat similar analysis of a probe string in Schwarzschild-AdS background.

What is a *nonlinear* realisation of the underlying time-reversal symmetry in the ingoing EF coordinates? This could be worked out with the help of (3.10) and (3.11). The Fourier modes in the Schwarzschild and ingoing EF coordinates are related,

$$C_\mu(r, k) = \tilde{C}_\mu(r, k) e^{i\omega\zeta_s(r)}, \quad C_r(r, k) = \left[\tilde{C}_r(r, k) - \frac{\tilde{C}_t(r, k)}{f(r)} \right] e^{i\omega\zeta_s(r)},$$

$$r \in [r_h - \epsilon, \infty_s), \quad s = 1 \text{ or } 2, \quad (4.11)$$

where $\zeta_1(r)$ and $\zeta_2(r)$ are introduced in (3.3). Thus, in the ingoing EF coordinates, the time-reversal symmetry is realized as

$$\omega \rightarrow -\omega, \quad C_v(r, k) \rightarrow C_v(r, \bar{k}) e^{2i\omega\zeta_s(r)}, \quad C_i(r, k) \rightarrow -C_i(r, \bar{k}) e^{2i\omega\zeta_s(r)},$$

$$C_r(r, k) \rightarrow - \left[C_r(r, \bar{k}) + \frac{2C_v(r, \bar{k})}{f(r)} \right] e^{2i\omega\zeta_s(r)}, \quad s = 1, 2, \quad (4.12)$$

So far, no gauge choice has been specified. In [59], the EF radial gauge $C_r = 0$ was chosen, which is in tension with the linear realisation of the time-reversal symmetry (4.5). In fact, a time reversed solution is gauge transformed with respect to $C_r = 0$. Hence, in order to benefit from the simplicity of (4.5), we search for solutions in the Schwarzschild radial gauge $\tilde{C}_r = 0$.

The bulk EOMs (4.2)-(4.4) are also invariant under \mathcal{P} -symmetry (space inversion):

$$\vec{q} \rightarrow -\vec{q}, \quad \tilde{C}_t(r, k^\mu) \rightarrow \tilde{C}_t(r, -\bar{k}^\mu), \quad \tilde{C}_i(r, k^\mu) \rightarrow -\tilde{C}_i(r, -\bar{k}^\mu),$$

$$\tilde{C}_r(r, k^\mu) \rightarrow \tilde{C}_r(r, -\bar{k}^\mu), \quad (4.13)$$

or, alternatively, in the coordinate space (r, t, \vec{x})

$$\vec{x} \rightarrow -\vec{x}, \quad \tilde{C}_t(r, t, \vec{x}) \rightarrow \tilde{C}_t(r, t, -\vec{x}), \quad \tilde{C}_i(r, t, \vec{x}) \rightarrow -\tilde{C}_i(r, t, -\vec{x}),$$

$$\tilde{C}_r(r, t, \vec{x}) \rightarrow \tilde{C}_r(r, t, -\vec{x}). \quad (4.14)$$

Since the coordinate transformation from (3.1) to (3.2) does not involve spatial directions, the \mathcal{P} -symmetry in the EF coordinates takes exactly the same form as (4.13) and (4.14), which can be straightforwardly checked from the bulk EOMs (4.8)-(4.10).

The time-reversal \mathcal{T} symmetry and \mathcal{P} -symmetry help to examine the symmetry relations for TCFs in the effective action, as reviewed in subsection 2 B.

B. Horizon matching conditions

As has been already mentioned, we first derive independent solutions in the upper and lower segments, and then glue them at the surface $r = r_h - \epsilon$. In this way a complete solution valid along the whole radial contour in Figure 1 is constructed. A necessary element of this construction is a set of matching conditions for the bulk fields to be discussed in this subsection.

The contour in Figure 1 is cut along the surface $r = r_{\pm} \equiv r_h - \epsilon$, where the subscripts $+$ and $-$ are used to distinguish the upper and lower segments. Following [51], the matching conditions at $r = r_h - \epsilon$ can be obtained by demanding the total bulk action to be extremal with respect to variation of the horizon data $C_M(r_h - \epsilon, x^\mu)$. Consider variation of the bulk action³ (3.5)

$$\begin{aligned} \delta S_0 = & - \int d^4x \sqrt{-\gamma} n_M \delta C_N F^{MN} \Big|_{r_-}^{\infty_1} + \int d^4x \sqrt{-\gamma} n_M \delta C_N F^{MN} \Big|_{r_+}^{\infty_2} \\ & + \int d^4x \int_{\infty_2}^{\infty_1} dr \sqrt{-g} \left[\delta C_r \nabla_M F^{Mr} + \delta C_v \frac{\nabla_M F^{Mr}}{f(r)} \right] \end{aligned} \quad (4.15)$$

where we imposed the dynamical equations (3.16). The extremum condition (at the surface $r = r_h - \epsilon$) gives

$$\frac{\delta S}{\delta C_v(r_h - \epsilon)} = 0 \Rightarrow F^{rv}(r_+) - F^{rv}(r_-) = \lim_{\Delta \rightarrow 0} \int_{r_+ + \Delta}^{r_- - \Delta} dr \frac{\nabla_M F^{Mr}}{f(r)}, \quad (4.16)$$

$$\frac{\delta S}{\delta C_i(r_h - \epsilon)} = 0 \Rightarrow F^{ri}(r_+) - F^{ri}(r_-) = 0, \quad (4.17)$$

where Δ is an infinitesimal interval along the circle in Figure 1. The field strength components F^{ri} are continuous through the cutting surface. Yet, the F^{rv} component, being continuous for on-shell theory, may develop discontinuity if the constraint equation is relaxed, that is, $\nabla_M F^{Mr} \neq 0$. When implementing the Schwarzschild radial gauge $\tilde{C}_r = 0$, the matching condition (4.17) translates into

$$f(r) \partial_r C_i \Big|_{r=r_+} = f(r) \partial_r C_i \Big|_{r=r_-}. \quad (4.18)$$

³ The counter-term action $S_{\text{c.t.}}$ does not contribute to the variational problem near horizon.

Since $f(r)$ vanishes at the horizon, $\partial_r C_i$ may not be continuous. Similarly, C_r component is discontinuous.

The condition (4.16) is very non-trivial. It suggests that $\partial_r C_v$ is discontinuous too. Yet, this conclusion is based on assumption that C_μ is continuous across the cutting slice:

$$C_\mu(r_-) = C_\mu(r_+). \quad (4.19)$$

(4.19) is a natural choice that could be realised via a residual gauge transformation implementable on each segment independently. Furthermore, thanks to the residual gauge freedom, we could set

$$C_v(r_h - \epsilon, x^\mu) = 0. \quad (4.20)$$

This choice has been also implemented in [59], though through a somewhat different chain of arguments. Once the condition (4.20) is imposed, (4.16) fixes the discontinuity of $\partial_r C_v$ uniquely. Below we will construct the full solution of EOMs with the matching condition (4.20) and then check that (4.16) is indeed satisfied. This consistency check will be presented in Appendix B.

Finally, an added value of the choice (4.20) is that it makes the horizon contribution to the effective action S_0 vanish. Hence, (3.20) is correct ⁴.

C. Linearly independent solutions

In this subsection, we derive and analyse all linearly independent solutions of the dynamical EOMs (3.16) in a single Schwarzschild-AdS₅. The solutions are equally valid both in the upper and lower segments in Figure 1. As argued previously, in order to benefit from the linear realisation (4.5) of the time-reversal symmetry, we temporarily work in the Schwarzschild coordinate system combined with the Schwarzschild radial gauge. Eventually, linearly independent solutions in the ingoing EF coordinates will be deduced via the transformation rule (4.11). Without loss of generality, the spatial momentum \vec{q} is taken to be along the x -direction. Then, the bulk fields \tilde{C}_μ decouple between two sectors: the transverse sector $\tilde{C}_\perp = \{\tilde{C}_y, \tilde{C}_z\}$ and the longitudinal sector $\tilde{C}_\parallel = \{\tilde{C}_t, \tilde{C}_x\}$.

⁴ Working with another residual gauge would lead us to different matching conditions and, as a consequence, different solutions of the EOMs, and also to a modified expression for the effective action. The final action is however gauge invariant and hence should not depend on a particular choice of the residual gauge.

Transverse sector.

The transverse mode \tilde{C}_\perp obeys a single ODE:

$$0 = \partial_r[r f(r) \partial_r \tilde{C}_\perp] + \frac{\omega^2 r}{f(r)} \tilde{C}_\perp - q^2 r^{-1} \tilde{C}_\perp, \quad \perp = y, z. \quad (4.21)$$

Eq. (4.21) has two independent solutions distinguishable by their near horizon behaviour.

Near the horizon $r = r_h$, the ingoing solution $\tilde{C}_\perp^{\text{ig}}(r, k^\mu)$ behaves as

$$\tilde{C}_\perp^{\text{ig}}(r, k^\mu) \xrightarrow{r \rightarrow r_h} (r - r_h)^{-i\omega/(4r_h)} \left[\tilde{C}_\perp^h + \tilde{C}_\perp^1 (r - r_h) + \tilde{C}_\perp^2 (r - r_h)^2 + \dots \right], \quad (4.22)$$

where \tilde{C}_\perp^h is an integration constant (initial condition), which we refer to as horizon data.

The remaining coefficients $\tilde{C}_\perp^1, \tilde{C}_\perp^2, \dots$ are uniquely fixed in terms of \tilde{C}_\perp^h .

The outgoing solution⁵ $\tilde{C}_\perp^{\text{og}}(r, k^\mu)$ is obtained from the ingoing one by the time-reversal symmetry (4.5)

$$\tilde{C}_\perp^{\text{og}}(r, k^\mu) = -\tilde{C}_\perp^{\text{ig}}(r, \bar{k}^\mu). \quad (4.23)$$

Both solutions are functions of q^2 as is obvious from (4.21), and hence they are \mathcal{P} -invariant.

From (4.11), the solutions in the ingoing EF coordinates read:

$$C_\perp^{\text{ig}}(r, k^\mu) = \tilde{C}_\perp^{\text{ig}}(r, k^\mu) e^{i\omega\zeta_s(r)}, \quad C_\perp^{\text{og}}(r, k^\mu) = \tilde{C}_\perp^{\text{og}}(r, k^\mu) e^{i\omega\zeta_s(r)}, \quad r \in [r_h - \epsilon, \infty_s). \quad (4.24)$$

Thus, the ingoing and outgoing solutions are related to each other via

$$C_\perp^{\text{og}}(r, k^\mu) = -C_\perp^{\text{ig}}(r, \bar{k}^\mu) e^{2i\omega\zeta_s(r)}, \quad r \in [r_h - \epsilon, \infty_s), \quad s = 1 \text{ or } 2, \quad (4.25)$$

where (4.23) is used.

Near the AdS boundary the ingoing solution C_\perp^{ig} can be expanded

$$C_\perp^{\text{ig}}(r, k^\mu) \xrightarrow{r \rightarrow \infty} C_\perp^{\text{ig}(0)}(k^\mu) - \frac{i\omega C_\perp^{\text{ig}(0)}(k^\mu)}{r} + \frac{1}{2}(\omega^2 - q^2) C_\perp^{\text{ig}(0)}(k^\mu) \frac{\log r}{r^2} + \frac{C_\perp^{\text{ig}(2)}(k^\mu)}{r^2} + \dots \quad (4.26)$$

In principle, one could tune \tilde{C}_\perp^h so that $C_\perp^{\text{ig}(0)}(k^\mu) = 1$, though for a while we prefer to keep it unspecified.

⁵ The outgoing solution can be identified with the Hawking radiation.

Longitudinal sector.

The EOMs for the longitudinal sector $\tilde{C}_\parallel = \{\tilde{C}_t, \tilde{C}_x\}$ are

$$\begin{aligned} 0 &= \partial_r(r^3 \partial_r \tilde{C}_t) - \frac{r}{f(r)}(q^2 \tilde{C}_t + \omega q \tilde{C}_x), \\ 0 &= \partial_r[r f(r) \partial_r \tilde{C}_x] + \frac{r}{f(r)}(\omega^2 \tilde{C}_x + \omega q \tilde{C}_t). \end{aligned} \quad (4.27)$$

Compared to the transverse case, the coupling between \tilde{C}_t and \tilde{C}_x makes the longitudinal sector much more involved. The system of coupled equations (4.27) has four linearly independent solutions, which could be differentiated by their near horizon behaviour.

- The first solution is the ingoing solution $\{\tilde{C}_t^{\text{ig}}, \tilde{C}_x^{\text{ig}}\}$,

$$\begin{aligned} \tilde{C}_t^{\text{ig}}(r, k^\mu) &\xrightarrow{r \rightarrow r_h} (r - r_h)^{1 - i\omega/(4r_h)} \left[\frac{4iq \tilde{C}_x^{\text{ig}h}}{4r_h^2 - i\omega r_h} + \dots \right], \\ \tilde{C}_x^{\text{ig}}(r, k^\mu) &\xrightarrow{r \rightarrow r_h} (r - r_h)^{-i\omega/(4r_h)} \left[\tilde{C}_x^{\text{ig}h} + \frac{i\omega \tilde{C}_x^{\text{ig}h} (8r_h^2 + 2i\omega r_h + \omega^2 - 4q^2)}{8r_h^2 (8r_h^2 - 6i\omega r_h - \omega^2)} (r - r_h) + \dots \right], \end{aligned} \quad (4.28)$$

where \dots are higher powers of $(r - r_h)$. Both functions $\{\tilde{C}_t^{\text{ig}}, \tilde{C}_x^{\text{ig}}\}$ are uniquely determined in terms of single horizon data $\tilde{C}_x^{\text{ig}h}$. It is important to observe that \tilde{C}_t^{ig} is an odd function of q while \tilde{C}_x^{ig} is even.

- The second solution of (4.27) is the outgoing solution $\{\tilde{C}_t^{\text{og}}, \tilde{C}_x^{\text{og}}\}$, which is obtained from the ingoing solution by the time-reversal transformation (4.5)

$$\tilde{C}_t^{\text{og}}(r, k^\mu) = \tilde{C}_t^{\text{ig}}(r, \bar{k}^\mu), \quad \tilde{C}_x^{\text{og}}(r, k^\mu) = -\tilde{C}_x^{\text{ig}}(r, \bar{k}^\mu). \quad (4.29)$$

- The third solution is the pure gauge (pg) solution [12]:

$$\tilde{C}_t^{\text{pg}}(r, k^\mu) = -i\omega \tilde{\Lambda}(k^\mu), \quad \tilde{C}_x^{\text{pg}}(r, k^\mu) = iq \tilde{\Lambda}(k^\mu), \quad (4.30)$$

where $\tilde{\Lambda}(k^\mu)$ is an r -independent gauge parameter of the residual gauge symmetry. As we have argued above, $\tilde{C}_t = 0$ at the horizon can be imposed as a residual gauge fixing. This choice of the gauge is equivalent to setting $\tilde{\Lambda} = 0$.

- The fourth solution is the polynomial (pn) solution $\{\tilde{C}_t^{\text{pn}}, \tilde{C}_x^{\text{pn}}\}$. Near horizon it has a Taylor expansion in powers of $(r - r_h)$:

$$\tilde{C}_t^{\text{pn}}(r, k^\mu) \xrightarrow{r \rightarrow r_h} (r - r_h) \left[\tilde{C}_t^{\text{pn}h} + \frac{\tilde{C}_t^{\text{pn}h} (4q^2 - 48r_h^2 - 3\omega^2)}{2r_h (16r_h^2 + \omega^2)} (r - r_h) + \dots \right], \quad (4.31)$$

$$\tilde{C}_x^{\text{pn}}(r, k^\mu) \xrightarrow{r \rightarrow r_h} (r - r_h) \left[-\frac{\tilde{C}_t^{\text{pn}h} \omega q}{16r_h^2 + \omega^2} - \frac{\tilde{C}_t^{\text{pn}h} \omega q (4q^2 - 32r_h^2 - 3\omega^2)}{2r_h(16r_h^2 + \omega^2)(64r_h^2 + \omega^2)}(r - r_h) + \dots \right],$$

where \dots refer to terms that are uniquely fixed in terms of the horizon data $\tilde{C}_t^{\text{pn}h}$. Thus the boundary values of \tilde{C}_t^{pn} and \tilde{C}_x^{pn} are not independent. \tilde{C}_t^{pn} is a function of ω^2 and q^2 , that is, it is both \mathcal{T} and \mathcal{P} even. Similarly, because \tilde{C}_x^{pn} has an overall extra factor ωq , it is \mathcal{T} and \mathcal{P} invariant too.

Thus we have found all four linearly independent solutions. So far, they have been identified by their near horizon behaviours. In subsection 5B, we will also construct them numerically, for finite momenta. Under the rule (4.11), the linearly independent solutions in the ingoing EF coordinate are

$$\begin{aligned} C_{\parallel}^{\text{ig}}(r, k^\mu) &= \tilde{C}_{\parallel}^{\text{ig}}(r, k^\mu) e^{i\omega\zeta_s(r)}, & C_{\parallel}^{\text{og}}(r, k^\mu) &= \tilde{C}_{\parallel}^{\text{og}}(r, k^\mu) e^{i\omega\zeta_s(r)}, \\ C_{\parallel}^{\text{pg}}(r, k^\mu) &= \tilde{C}_{\parallel}^{\text{pg}}(r, k^\mu) e^{i\omega\zeta_s(r)}, & C_{\parallel}^{\text{pn}}(r, k^\mu) &= \tilde{C}_{\parallel}^{\text{pn}}(r, k^\mu) e^{i\omega\zeta_s(r)}, \end{aligned} \quad (4.32)$$

where $s = 2$ when $r \in [r_h - \epsilon, \infty_2)$ and $s = 1$ when $r \in [r_h - \epsilon, \infty_1)$. Here, the subscript \parallel collectively denotes the time component and x component of the bulk gauge field. Similarly as in the transverse case (4.25), the ingoing solution $\{C_v^{\text{ig}}, C_x^{\text{ig}}\}$ and the outgoing solution $\{C_v^{\text{og}}, C_x^{\text{og}}\}$ are related:

$$\begin{aligned} C_v^{\text{og}}(r, k^\mu) &= C_v^{\text{ig}}(r, \bar{k}^\mu) e^{2i\omega\zeta_s(r)}, & C_x^{\text{og}}(r, k^\mu) &= -C_x^{\text{ig}}(r, \bar{k}^\mu) e^{2i\omega\zeta_s(r)}, \\ r &\in [r_h - \epsilon, \infty_s), & s &= 1 \text{ or } 2. \end{aligned} \quad (4.33)$$

Near the AdS boundary the linearly independent solutions can be expanded

$$\begin{aligned} C_v^{\text{S}}(r, k^\mu) &\xrightarrow{r \rightarrow \infty} C_v^{\text{S}(0)}(k^\mu) - \frac{i\omega C_v^{\text{S}(0)}(k^\mu)}{r} + \frac{1}{2} \partial^\mu \mathcal{F}_{v\mu}^{\text{S}(0)}(k^\mu) \frac{\log r}{r^2} + \frac{C_v^{\text{S}(2)}(k^\mu)}{r^2} + \dots, \\ C_x^{\text{S}}(r, k^\mu) &\xrightarrow{r \rightarrow \infty} C_x^{\text{S}(0)}(k^\mu) - \frac{i\omega C_x^{\text{S}(0)}(k^\mu)}{r} + \frac{1}{2} \partial^\mu \mathcal{F}_{x\mu}^{\text{S}(0)}(k^\mu) \frac{\log r}{r^2} + \frac{C_x^{\text{S}(2)}(k^\mu)}{r^2} + \dots, \end{aligned} \quad (4.34)$$

where S stands for any of the three solutions, $S = (\text{ig}, \text{og}, \text{pn})$ and $\mathcal{F}^{\text{S}(0)}$ is the corresponding field strength. The expansion (4.34) is not valid for the pure gauge solution. In principle, one could tune the horizon data for each solution independently, so that $C_v^{\text{S}(0)}(k^\mu) = 1$. Then, there is no freedom left to also set $C_x^{\text{S}(0)}(k^\mu)$ to one: the value of $C_x^{\text{S}(0)}(k^\mu)$ would have to be determined from the dynamical equations.

It is important to notice that the solutions $\{\tilde{C}_t^{\text{ig}}, \tilde{C}_x^{\text{ig}}\}$, $\{\tilde{C}_t^{\text{og}}, \tilde{C}_x^{\text{og}}\}$, and $\{\tilde{C}_t^{\text{pg}}, \tilde{C}_x^{\text{pg}}\}$ satisfy the constraint equation (4.2) automatically, which makes it possible to relate the near

boundary expansions of these functions. Particularly,

$$\begin{aligned}\omega\tilde{C}_t^{S(2)}(k^\mu) + q\tilde{C}_x^{S(2)}(k^\mu) &= 0, \\ C_\mu^{S(0)}(k^\mu) &= \tilde{C}_\mu^{S(0)}(k^\mu), \quad C_\mu^{S(2)}(k^\mu) = \tilde{C}_\mu^{S(2)}(k^\mu) - \frac{1}{2}\omega^2\tilde{C}_\mu^{S(0)}(k^\mu),\end{aligned}\quad (4.35)$$

where the last two relations follows from (4.11). The polynomial solution, on the other hand, does not satisfy the constraint (4.2). Consequently, having the theory put on-shell is equivalent to setting the coefficient of the polynomial solution to zero.

D. Solutions over the entire radial contour: gluing at the horizon

In the previous subsection, we have found the independent solutions to dynamical EOMs (3.16) for a single copy of the doubled Schwarzschild-AdS₅. Our next task is to construct a full solution over the entire contour in Figure 1. To this end, the independent solutions on the upper and lower segments will be glued at the horizon, employing the matching conditions (4.18), (4.19) and (4.20) derived in subsection 4 B.

• Transverse sector.

The most general solution for C_\perp expressed in a piecewise form is:

$$\begin{aligned}C_\perp^{\text{up}}(r, k^\mu) &= c_\perp^{\text{up}}C_\perp^{\text{ig}}(r, k^\mu) - h_\perp^{\text{up}}C_\perp^{\text{ig}}(r, \bar{k}^\mu)e^{2i\omega\zeta_2(r)}, \quad r \in [r_h - \epsilon, \infty_2), \\ C_\perp^{\text{dw}}(r, k^\mu) &= c_\perp^{\text{dw}}C_\perp^{\text{ig}}(r, k^\mu) - h_\perp^{\text{dw}}C_\perp^{\text{ig}}(r, \bar{k}^\mu)e^{2i\omega\zeta_1(r)}, \quad r \in [r_h - \epsilon, \infty_1).\end{aligned}\quad (4.36)$$

Here $c_\perp^{\text{up,dw}} = c_\perp^{\text{up,dw}}(k_\mu)$ and $h_\perp^{\text{up,dw}} = h_\perp^{\text{up,dw}}(k_\mu)$ are linear superposition coefficients. Near the horizon, C_\perp^{ig} is regular while C_\perp^{og} oscillates as $e^{2i\omega\zeta_1(r)}$ in the upper segment and as $e^{2i\omega\zeta_2(r)}$ in the lower one. The matching condition (4.18) and the continuity condition (4.19) imply

$$h_\perp^{\text{up}} = h_\perp^{\text{dw}}e^{\beta\omega}, \quad c_\perp^{\text{up}} = c_\perp^{\text{dw}}. \quad (4.37)$$

Eventually, the solution for the transverse mode is

$$\begin{aligned}C_\perp^{\text{up}}(r, k^\mu) &= c_\perp C_\perp^{\text{ig}}(r, k^\mu) - h_\perp C_\perp^{\text{ig}}(r, \bar{k}^\mu)e^{2i\omega\zeta_2(r)}, \quad r \in [r_h - \epsilon, \infty_2), \\ C_\perp^{\text{dw}}(r, k^\mu) &= c_\perp C_\perp^{\text{ig}}(r, k^\mu) - h_\perp e^{-\beta\omega} C_\perp^{\text{ig}}(r, \bar{k}^\mu)e^{2i\omega\zeta_1(r)}, \quad r \in [r_h - \epsilon, \infty_1),\end{aligned}\quad (4.38)$$

where $c_\perp^{\text{up}} \rightarrow c_\perp$ and $h_\perp^{\text{up}} \rightarrow h_\perp$ relabelling was made. The piecewise solution (4.38) could be put into a more compact form:

$$C_\perp(r, k^\mu) = c_\perp C_\perp^{\text{ig}}(r, k^\mu) - h_\perp C_\perp^{\text{ig}}(r, \bar{k}^\mu)e^{2i\omega\zeta(r)}, \quad r \in (\infty_2, \infty_1), \quad (4.39)$$

where $\zeta(r)$ is defined similarly to $\zeta_2(r)$ but with the r interval extended over the whole contour:

$$\zeta(r) \equiv \int_{\infty_2}^r \frac{dy}{f(y)}, \quad r \in (\infty_2, \infty_1). \quad (4.40)$$

The decomposition coefficients c_\perp and h_\perp are fixed from the boundary conditions at $r = \infty_1$ and $r = \infty_2$ (see (4.26)).

$$\begin{aligned} c_\perp C_\perp^{\text{ig}(0)}(k^\mu) - h_\perp C_\perp^{\text{ig}(0)}(\bar{k}^\mu) &= B_{2\perp}(k^\mu), \\ c_\perp C_\perp^{\text{ig}(0)}(k^\mu) - h_\perp e^{-\beta\omega} C_\perp^{\text{ig}(0)}(\bar{k}^\mu) &= B_{1\perp}(k^\mu), \\ \Rightarrow c_\perp &= \frac{1}{2} \coth \frac{\beta\omega}{2} \frac{B_{a\perp}(k^\mu)}{C_\perp^{\text{ig}(0)}(k^\mu)} + \frac{B_{r\perp}(k^\mu)}{C_\perp^{\text{ig}(0)}(k^\mu)} \quad h_\perp = \frac{B_{a\perp}(k^\mu)}{(1 - e^{-\beta\omega}) C_\perp^{\text{ig}(0)}(\bar{k}^\mu)}. \end{aligned} \quad (4.41)$$

As mentioned earlier, $C_\perp^{\text{ig}(0)}$ can be set to one without loss of generality.

• Longitudinal sector

With the four independent solutions presented in subsection 4 C, we construct the most general solution for the longitudinal sector $\{C_v, C_x\}$ in a piecewise form:

$$\begin{aligned} C_v^{\text{up}}(r, k^\mu) &= c_\parallel^{\text{up}} C_v^{\text{ig}}(r, k^\mu) + h_\parallel^{\text{up}} C_v^{\text{ig}}(r, \bar{k}^\mu) e^{2i\omega\zeta_2(r)} + p_\parallel^{\text{up}} C_v^{\text{pg}}(r, k^\mu) \\ &\quad + n_\parallel^{\text{up}} C_v^{\text{pn}}(r, k^\mu), \quad r \in [r_h - \epsilon, \infty_2), \\ C_x^{\text{up}}(r, k^\mu) &= c_\parallel^{\text{up}} C_x^{\text{ig}}(r, k^\mu) - h_\parallel^{\text{up}} C_x^{\text{ig}}(r, \bar{k}^\mu) e^{2i\omega\zeta_2(r)} + p_\parallel^{\text{up}} C_x^{\text{pg}}(r, k^\mu) \\ &\quad + n_\parallel^{\text{up}} C_x^{\text{pn}}(r, k^\mu), \quad r \in [r_h - \epsilon, \infty_2), \\ C_v^{\text{dw}}(r, k^\mu) &= c_\parallel^{\text{dw}} C_v^{\text{ig}}(r, k^\mu) + h_\parallel^{\text{dw}} C_v^{\text{ig}}(r, \bar{k}^\mu) e^{2i\omega\zeta_1(r)} + p_\parallel^{\text{dw}} C_v^{\text{pg}}(r, k^\mu) \\ &\quad + n_\parallel^{\text{dw}} C_v^{\text{pn}}(r, k^\mu), \quad r \in [r_h - \epsilon, \infty_1), \\ C_x^{\text{dw}}(r, k^\mu) &= c_\parallel^{\text{dw}} C_x^{\text{ig}}(r, k^\mu) - h_\parallel^{\text{dw}} C_x^{\text{ig}}(r, \bar{k}^\mu) e^{2i\omega\zeta_1(r)} + p_\parallel^{\text{dw}} C_x^{\text{pg}}(r, k^\mu) \\ &\quad + n_\parallel^{\text{dw}} C_x^{\text{pn}}(r, k^\mu), \quad r \in [r_h - \epsilon, \infty_1), \end{aligned} \quad (4.42)$$

where $\{C_v^{\text{ig}}, C_x^{\text{ig}}\}$, $\{C_v^{\text{pg}}, C_x^{\text{pg}}\}$ and $\{C_v^{\text{pn}}, C_x^{\text{pn}}\}$ are related to the solutions in the Schwarzschild coordinates by the rule (4.32). Next, the piecewise solutions (4.42) are glued via the matching conditions (4.19), (4.18), and (4.20). At the horizon surface, both C_v^{ig} and C_v^{pn} vanish, while C_v^{pg} is generically nonzero. Thus, the condition (4.20) requires⁶

$$p_\parallel^{\text{up}} = p_\parallel^{\text{dw}} = 0. \quad (4.43)$$

⁶ In fact, $p_\parallel^{\text{up}, \text{dw}}$ can be absorbed into redefinition of $\tilde{\Lambda}$ in (4.30).

The condition (4.18) implies

$$h_{\parallel}^{\text{up}} = h_{\parallel}^{\text{dw}} e^{\beta\omega}, \quad (4.44)$$

where we have used the fact that

$$\begin{aligned} f(r) \partial_r C_x^{\text{ig}}(r, k^\mu) &\xrightarrow{r \rightarrow r_h} 0, & f(r) \partial_r C_x^{\text{pn}}(r, k^\mu) &\xrightarrow{r \rightarrow r_h} 0, \\ f(r) \partial_r C_x^{\text{og}}(r, k^\mu) &\xrightarrow{r \rightarrow r_h} -2i\omega C_x^{\text{ig}}(r, \bar{k}^\mu) e^{2i\omega\zeta_1(r)}, & r &\in [r_h - \epsilon, \infty_1), \\ f(r) \partial_r C_x^{\text{og}}(r, k^\mu) &\xrightarrow{r \rightarrow r_h} -2i\omega C_x^{\text{ig}}(r, \bar{k}^\mu) e^{2i\omega\zeta_2(r)}, & r &\in [r_h - \epsilon, \infty_2). \end{aligned} \quad (4.45)$$

Finally, the matching condition (4.19) implies

$$c_{\parallel}^{\text{up}} = c_{\parallel}^{\text{dw}}. \quad (4.46)$$

Eventually, the entire solution for the longitudinal sector is

$$\begin{aligned} C_v^{\text{up}}(r, k^\mu) &= c_{\parallel} C_v^{\text{ig}}(r, k^\mu) + h_{\parallel} C_v^{\text{ig}}(r, \bar{k}^\mu) e^{2i\omega\zeta_2(r)} + n_{\parallel}^{\text{up}} C_v^{\text{pn}}(r, k^\mu), \\ C_x^{\text{up}}(r, k^\mu) &= c_{\parallel} C_x^{\text{ig}}(r, k^\mu) - h_{\parallel} C_x^{\text{ig}}(r, \bar{k}^\mu) e^{2i\omega\zeta_2(r)} + n_{\parallel}^{\text{up}} C_x^{\text{pn}}(r, k^\mu), \\ C_v^{\text{dw}}(r, k^\mu) &= c_{\parallel} C_v^{\text{ig}}(r, k^\mu) + h_{\parallel} e^{-\beta\omega} C_v^{\text{ig}}(r, \bar{k}^\mu) e^{2i\omega\zeta_1(r)} + n_{\parallel}^{\text{dw}} C_v^{\text{pn}}(r, k^\mu), \\ C_x^{\text{dw}}(r, k^\mu) &= c_{\parallel} C_x^{\text{ig}}(r, k^\mu) - h_{\parallel} e^{-\beta\omega} C_x^{\text{ig}}(r, \bar{k}^\mu) e^{2i\omega\zeta_1(r)} + n_{\parallel}^{\text{dw}} C_x^{\text{pn}}(r, k^\mu), \end{aligned} \quad (4.47)$$

where $c_{\parallel}^{\text{up}} \rightarrow c_{\parallel}$, $h_{\parallel}^{\text{up}} \rightarrow h_{\parallel}$ relabelling is made. Due to the presence of the polynomial solution $\{C_v^{\text{pn}}, C_x^{\text{pn}}\}$, it is not possible to cast the final result (4.47) into a more compact form, similar to (4.39).

Recall that near the AdS boundary all the linearly independent solutions have asymptotic expansions similar to the general case (3.22) and (3.23), cf. (4.34). The coefficients $c_{\parallel}, h_{\parallel}, n_{\parallel}^{\text{dw}}, n_{\parallel}^{\text{up}}$ in (4.47) are fixed by the AdS boundary conditions

$$\begin{aligned} c_{\parallel} C_v^{\text{ig}(0)}(k^\mu) + h_{\parallel} C_v^{\text{ig}(0)}(\bar{k}^\mu) + n_{\parallel}^{\text{up}} C_v^{\text{pn}(0)}(k^\mu) &= B_{2v}(k^\mu), \\ c_{\parallel} C_x^{\text{ig}(0)}(k^\mu) - h_{\parallel} C_x^{\text{ig}(0)}(\bar{k}^\mu) + n_{\parallel}^{\text{up}} C_x^{\text{pn}(0)}(k^\mu) &= B_{2x}(k^\mu), \\ c_{\parallel} C_v^{\text{ig}(0)}(k^\mu) + h_{\parallel} e^{-\beta\omega} C_v^{\text{ig}(0)}(\bar{k}^\mu) + n_{\parallel}^{\text{dw}} C_v^{\text{pn}(0)}(k^\mu) &= B_{1v}(k^\mu), \\ c_{\parallel} C_x^{\text{ig}(0)}(k^\mu) - h_{\parallel} e^{-\beta\omega} C_x^{\text{ig}(0)}(\bar{k}^\mu) + n_{\parallel}^{\text{dw}} C_x^{\text{pn}(0)}(k^\mu) &= B_{1x}(k^\mu), \end{aligned} \quad (4.48)$$

which yield

$$c_{\parallel} = \frac{1}{2} G_1^{-1} \{ 2B_{rx}(k^\mu) C_v^{\text{pn}(0)}(k^\mu) - 2B_{rv}(k^\mu) C_x^{\text{pn}(0)}(k^\mu) \}$$

$$+ \coth \frac{\beta\omega}{2} \left[B_{ax}(\omega, q) C_v^{\text{pn}(0)}(k^\mu) - B_{av}(k^\mu) C_x^{\text{pn}(0)}(k^\mu) \right] \Big\}, \quad (4.49)$$

$$h_{\parallel} = (1 - e^{-\beta\omega})^{-1} G_2^{-1} \left[B_{ax}(k^\mu) C_v^{\text{pn}(0)}(k^\mu) - B_{av}(k^\mu) C_x^{\text{pn}(0)}(k^\mu) \right], \quad (4.50)$$

$$n_{\parallel}^{\text{dw}} - n_{\parallel}^{\text{up}} = G_2^{-1} \left[B_{ax}(k^\mu) C_v^{\text{ig}(0)}(\bar{k}^\mu) + B_{av}(k^\mu) C_x^{\text{ig}(0)}(\bar{k}^\mu) \right], \quad (4.51)$$

$$\begin{aligned} \frac{1}{2}(n_{\parallel}^{\text{dw}} + n_{\parallel}^{\text{up}}) &= -G_1^{-1} \left[B_{rx}(k^\mu) C_v^{\text{ig}(0)}(k^\mu) - B_{rv}(k^\mu) C_x^{\text{ig}(0)}(k^\mu) \right] - \frac{1}{2} \coth \frac{\beta\omega}{2} \\ &\times G_1^{-1} G_2^{-1} G_3 \left[B_{ax}(k^\mu) C_v^{\text{pn}(0)}(k^\mu) - B_{av}(k^\mu) C_x^{\text{pn}(0)}(k^\mu) \right], \end{aligned} \quad (4.52)$$

where

$$\begin{aligned} G_1 &= C_v^{\text{pn}(0)}(k^\mu) C_x^{\text{ig}(0)}(k^\mu) - C_v^{\text{ig}(0)}(k^\mu) C_x^{\text{pn}(0)}(k^\mu), \\ G_2 &= C_v^{\text{pn}(0)}(k^\mu) C_x^{\text{ig}(0)}(\bar{k}^\mu) + C_v^{\text{ig}(0)}(\bar{k}^\mu) C_x^{\text{pn}(0)}(k^\mu), \\ G_3 &= C_v^{\text{ig}(0)}(\bar{k}^\mu) C_x^{\text{ig}(0)}(k^\mu) + C_v^{\text{ig}(0)}(k^\mu) C_x^{\text{ig}(0)}(\bar{k}^\mu). \end{aligned} \quad (4.53)$$

Notice that $G_2 = G_1^*$. Without loss of generality two of the coefficients, say, $C_v^{\text{pn}(0)}$ and $C_v^{\text{ig}(0)}$ could be set to one. The remaining coefficients would have to be found from the solutions of the EOMs. Finally, it is not difficult to verify that $G_1 \neq 0$.

E. From the bulk solutions to the effective action

With the entire solution for $C_M(r, v, \vec{x})$ derived in subsection 4D, we are now ready to evaluate the effective Lagrangian (3.24), which can be split into transverse and longitudinal parts:

$$\mathcal{L}_{\text{eff}} = \mathcal{L}_{\text{eff}}^{\perp} + \mathcal{L}_{\text{eff}}^{\parallel} \quad (4.54)$$

We will need near-boundary expansion coefficients $C_M^{(2)}$ and the expansion of $e^{2i\omega\zeta_s(r)}$:

$$e^{2i\omega\zeta_s(r)} \xrightarrow{r \rightarrow \infty_s} 1 - \frac{2i\omega}{r} - \frac{2\omega^2}{r^2} + \dots, \quad s = 1, \text{ or } 2. \quad (4.55)$$

• $\mathcal{L}_{\text{eff}}^{\perp}$

In the (r, a) -basis, the coefficients $C_{\perp}^{(2)}$ (normalizable modes) are

$$C_{a\perp}^{(2)}(k^\mu) = - \frac{C_{\perp}^{\text{ig}(2)}(\bar{k}^\mu)}{C_{\perp}^{\text{ig}(0)}(\bar{k}^\mu)} B_{a\perp}(k^\mu), \quad (4.56)$$

$$C_{r\perp}^{(2)}(k^\mu) = \frac{1}{2} \coth \frac{\beta\omega}{2} \left[\frac{C_{\perp}^{\text{ig}(2)}(k^\mu)}{C_{\perp}^{\text{ig}(0)}(k^\mu)} - \frac{C_{\perp}^{\text{ig}(2)}(\bar{k}^\mu)}{C_{\perp}^{\text{ig}(0)}(\bar{k}^\mu)} \right] B_{a\perp}(k^\mu) + \frac{C_{\perp}^{\text{ig}(2)}(k^\mu)}{C_{\perp}^{\text{ig}(0)}(k^\mu)} B_{r\perp}(k^\mu). \quad (4.57)$$

From (3.24), the transverse part of the effective Lagrangian is

$$\mathcal{L}_{\text{eff}}^\perp = B_{r\perp}(x)C_{a\perp}^{(2)}(x) + B_{a\perp}(x)C_{r\perp}^{(2)}(x) - \frac{1}{2}B_{a\perp}(x)\partial_v^2 B_{r\perp}(x) - \frac{1}{2}B_{a\perp}(x)\vec{\partial}^2 B_{r\perp}(x), \quad (4.58)$$

which in the momentum space reads

$$\begin{aligned} \mathcal{L}_{\text{eff}}^\perp(k) = & B_{a\perp}(-k) \left[\frac{2C_{\perp}^{\text{ig}(2)}(k)}{C_{\perp}^{\text{ig}(0)}(k)} + \frac{1}{2}\omega^2 + \frac{1}{2}q^2 \right] B_{r\perp}(k) \\ & + B_{a\perp}(-k) \frac{1}{2} \coth \frac{\beta\omega}{2} \left[\frac{C_{\perp}^{\text{ig}(2)}(k)}{C_{\perp}^{\text{ig}(0)}(k)} - \frac{C_{\perp}^{\text{ig}(2)}(\bar{k})}{C_{\perp}^{\text{ig}(0)}(\bar{k})} \right] B_{a\perp}(k). \end{aligned} \quad (4.59)$$

Comparing (4.59) with (2.2), the TCFs in (2.2) are expressed in terms of the results obtained in the bulk:

$$-i\omega w_8(k) + q^2 w_9(k) = \frac{2C_{\perp}^{\text{ig}(2)}(k)}{C_{\perp}^{\text{ig}(0)}(k)} + \frac{1}{2}\omega^2 + \frac{1}{2}q^2, \quad (4.60)$$

$$\frac{i}{2}w_2(k) = \frac{1}{2} \coth \frac{\beta\omega}{2} \left[\frac{C_{\perp}^{\text{ig}(2)}(k)}{C_{\perp}^{\text{ig}(0)}(k)} - \frac{C_{\perp}^{\text{ig}(2)}(\bar{k})}{C_{\perp}^{\text{ig}(0)}(\bar{k})} \right]. \quad (4.61)$$

While w_2 is determined entirely by the transverse sector, the coefficients w_8, w_9 will be uniquely fixed only with addition of the longitudinal sector.

• $\mathcal{L}_{\text{eff}}^\parallel$

In order to cast the results into a more compact form, the following ratios are introduced

$$\begin{aligned} R_v^{\text{ig}}(k) &= \frac{C_v^{\text{ig}(2)}(k)}{C_v^{\text{ig}(0)}(k)}, & R_v^{\text{pn}}(k) &= \frac{C_v^{\text{pn}(2)}(k)}{C_v^{\text{pn}(0)}(k)}, & R_{xv}^{\text{ig}}(k) &= \frac{C_x^{\text{ig}(2)}(k)}{C_v^{\text{ig}(0)}(k)}, \\ R_{xv}^{\text{pn}}(k) &= \frac{C_x^{\text{pn}(2)}(k)}{C_v^{\text{pn}(0)}(k)}, & \bar{R}_{xv}^{\text{ig}}(k) &= \frac{C_x^{\text{ig}(0)}(k)}{C_v^{\text{ig}(0)}(k)}, & \bar{R}_{xv}^{\text{pn}}(k) &= \frac{C_x^{\text{pn}(0)}(k)}{C_v^{\text{pn}(0)}(k)}. \end{aligned} \quad (4.62)$$

These ratios are determined by solving the dynamical EOMs (3.16) in a single copy of doubled Schwarzschild-AdS₅, see subsection 4 C. It is important to recall that $C_v^{\text{ig}(2)}$ is related to $C_x^{\text{ig}(2)}$ via (4.35). Furthermore, there is still the freedom to set both $C_v^{\text{ig}(0)}$ and $C_v^{\text{pn}(0)}$ to one.

Near the AdS boundaries $r = \infty_1$ and $r = \infty_2$, we extract the normalizable modes in C_v and C_x (in the (r, a) -basis):

$$C_{rv}^{(2)}(k) = c_\parallel C_v^{\text{ig}(2)}(k) + \frac{1}{2}h_\parallel(1 + e^{-\beta\omega})C_v^{\text{ig}(2)}(\bar{k}) + \frac{1}{2}(n_\parallel^{\text{dw}} + n_\parallel^{\text{up}})C_v^{\text{pn}(2)}(k)$$

$$\begin{aligned}
&= \frac{R_v^{\text{ig}}(k) - R_v^{\text{pn}}(k)}{\bar{R}_{xv}^{\text{ig}}(k) - \bar{R}_{xv}^{\text{pn}}(k)} B_{rx}(k) + \frac{\bar{R}_{xv}^{\text{ig}}(k) R_v^{\text{pn}}(k) - \bar{R}_{xv}^{\text{pn}}(k) R_v^{\text{ig}}(k)}{\bar{R}_{xv}^{\text{ig}}(k) - \bar{R}_{xv}^{\text{pn}}(k)} B_{rv}(k) \\
&\quad + \frac{1}{2} \coth \frac{\beta\omega}{2} \left\{ \frac{R_v^{\text{ig}}(k) - R_v^{\text{pn}}(k)}{\bar{R}_{xv}^{\text{ig}}(k) - \bar{R}_{xv}^{\text{pn}}(k)} + \frac{R_v^{\text{ig}}(\bar{k}) - R_v^{\text{pn}}(k)}{\bar{R}_{xv}^{\text{ig}}(\bar{k}) + \bar{R}_{xv}^{\text{pn}}(k)} \right\} [B_{ax}(k) - \bar{R}_{xv}^{\text{pn}}(k) B_{av}(k)],
\end{aligned} \tag{4.63}$$

$$\begin{aligned}
C_{av}^{(2)}(k) &= -h_{\parallel}(1 - e^{-\beta\omega}) C_v^{\text{ig}(2)}(\bar{k}) + (n_{\parallel}^{\text{dw}} - n_{\parallel}^{\text{up}}) C_v^{\text{pn}(2)}(k) \\
&= R_v^{\text{pn}}(k) \frac{B_{ax}(k) + \bar{R}_{xv}^{\text{ig}}(\bar{k}) B_{av}(k)}{\bar{R}_{xv}^{\text{ig}}(\bar{k}) + \bar{R}_{xv}^{\text{pn}}(k)} + R_v^{\text{ig}}(\bar{k}) \frac{-B_{ax}(k) + \bar{R}_{xv}^{\text{pn}}(k) B_{av}(k)}{\bar{R}_{xv}^{\text{ig}}(\bar{k}) + \bar{R}_{xv}^{\text{pn}}(k)},
\end{aligned} \tag{4.64}$$

$$\begin{aligned}
C_{rx}^{(2)}(k) &= c_{\parallel} C_x^{\text{ig}(2)}(k) - \frac{1}{2} h_{\parallel} (1 + e^{-\beta\omega}) C_x^{\text{ig}(2)}(\bar{k}) + \frac{1}{2} (n_{\parallel}^{\text{dw}} + n_{\parallel}^{\text{up}}) C_x^{\text{pn}(2)}(k) \\
&= R_{xv}^{\text{ig}}(k) \frac{B_{rx}(k) - \bar{R}_{xv}^{\text{ig}}(k) B_{rv}(k)}{\bar{R}_{xv}^{\text{ig}}(k) - \bar{R}_{xv}^{\text{pn}}(k)} + R_{xv}^{\text{ig}}(k) \frac{-B_{rx}(k) + \bar{R}_{xv}^{\text{ig}}(k) B_{rv}(k)}{\bar{R}_{xv}^{\text{ig}}(k) - \bar{R}_{xv}^{\text{pn}}(k)} \\
&\quad + \frac{1}{2} \coth \frac{\beta\omega}{2} \left\{ \frac{R_{xv}^{\text{ig}}(k) - R_{xv}^{\text{pn}}(k)}{\bar{R}_{xv}^{\text{ig}}(k) - \bar{R}_{xv}^{\text{pn}}(k)} - \frac{R_{xv}^{\text{ig}}(\bar{k}) + R_{xv}^{\text{pn}}(k)}{\bar{R}_{xv}^{\text{ig}}(\bar{k}) + \bar{R}_{xv}^{\text{pn}}(k)} \right\} [B_{ax}(k) - \bar{R}_{xv}^{\text{pn}}(k) B_{av}(k)],
\end{aligned} \tag{4.65}$$

$$\begin{aligned}
C_{ax}^{(2)}(k) &= h_{\parallel}(1 - e^{-\beta\omega}) C_x^{\text{ig}(2)}(\bar{k}) + (n_{\parallel}^{\text{dw}} - n_{\parallel}^{\text{up}}) C_x^{\text{pn}(2)}(k) \\
&= R_{xv}^{\text{ig}}(\bar{k}) \frac{B_{ax}(k) - \bar{R}_{xv}^{\text{pn}}(k) B_{av}(k)}{\bar{R}_{xv}^{\text{ig}}(\bar{k}) + \bar{R}_{xv}^{\text{pn}}(k)} + R_{xv}^{\text{pn}}(k) \frac{B_{ax}(k) + \bar{R}_{xv}^{\text{ig}}(\bar{k}) B_{av}(k)}{\bar{R}_{xv}^{\text{ig}}(\bar{k}) + \bar{R}_{xv}^{\text{pn}}(k)}.
\end{aligned} \tag{4.66}$$

From (3.24), the longitudinal part of the effective Lagrangian is

$$\begin{aligned}
\mathcal{L}_{\text{eff}}^{\parallel} &= -B_{rv}(x) C_{av}^{(2)}(x) - B_{av}(x) C_{rv}^{(2)}(x) + B_{rx}(x) C_{ax}^{(2)}(x) + B_{ax} C_{rx}^{(2)}(x) \\
&\quad + \frac{1}{2} \partial_x B_{ax}(x) \partial_v B_{rv}(x) - \frac{1}{2} B_{av}(x) \partial_v \partial_x B_{rx}(x) - \frac{1}{2} B_{ax}(x) \partial_v^2 B_{rx}(x) \\
&\quad + \frac{1}{2} B_{av}(x) \vec{\partial}^2 B_{rv}(x) + B_{av}(x) \partial_v^2 B_{rv}(x),
\end{aligned} \tag{4.67}$$

which in the momentum space becomes

$$\begin{aligned}
\mathcal{L}_{\text{eff}}^{\parallel}(k) &= B_{av}(-k) \frac{i}{2} w_1(k) B_{av}(k) + B_{ax}(-k) \left(\frac{i}{2} w_2(k) + \frac{i}{2} q^2 w_3(k) \right) B_{ax}(k) \\
&\quad + B_{av}(-k) [-q w_4(k)] B_{ax}(k) + B_{av}(-k) w_5(k) B_{rv}(k) \\
&\quad + B_{av}(-k) \omega q w_6(k) B_{rx}(k) + B_{ax}(-k) [-i q w_7(k)] B_{rv}(k) \\
&\quad + B_{ax}(-k) [-i \omega w_8(k)] B_{rx}(k),
\end{aligned} \tag{4.68}$$

with the TCFs given by the following expressions

$$\frac{i}{2} w_1(k) = \frac{1}{2} \coth \frac{\beta\omega}{2} \left[\frac{R_v^{\text{ig}}(k) - R_v^{\text{pn}}(k)}{\bar{R}_{xv}^{\text{ig}}(k) - \bar{R}_{xv}^{\text{pn}}(k)} + \frac{R_v^{\text{ig}}(\bar{k}) - R_v^{\text{pn}}(k)}{\bar{R}_{xv}^{\text{ig}}(\bar{k}) + \bar{R}_{xv}^{\text{pn}}(k)} \right] \bar{R}_{xv}^{\text{pn}}(k), \tag{4.69}$$

$$\frac{i}{2}w_2(k) + \frac{i}{2}q^2w_3(k) = \frac{1}{2}\coth\frac{\beta\omega}{2}\left[\frac{R_v^{\text{ig}}(k) - R_v^{\text{pn}}(k)}{\bar{R}_{xv}^{\text{ig}}(k) - \bar{R}_{xv}^{\text{pn}}(k)} - \frac{R_v^{\text{ig}}(\bar{k}) + R_v^{\text{pn}}(k)}{\bar{R}_{xv}^{\text{ig}}(\bar{k}) + \bar{R}_{xv}^{\text{pn}}(k)}\right], \quad (4.70)$$

$$\begin{aligned} -qw_4(k) = & -\frac{1}{2}\coth\frac{\beta\omega}{2}\left[\frac{R_v^{\text{ig}}(k) - R_v^{\text{pn}}(k)}{\bar{R}_{xv}^{\text{ig}}(k) - \bar{R}_{xv}^{\text{pn}}(k)} + \frac{R_v^{\text{ig}}(\bar{k}) - R_v^{\text{pn}}(k)}{\bar{R}_{xv}^{\text{ig}}(\bar{k}) + \bar{R}_{xv}^{\text{pn}}(k)}\right] \\ & + \frac{1}{2}\coth\frac{\beta\omega}{2}\left[\frac{R_{xv}^{\text{ig}}(\bar{k}) + R_{xv}^{\text{pn}}(k)}{\bar{R}_{xv}^{\text{ig}}(\bar{k}) + \bar{R}_{xv}^{\text{pn}}(k)} - \frac{R_{xv}^{\text{ig}}(k) - R_{xv}^{\text{pn}}(k)}{\bar{R}_{xv}^{\text{ig}}(k) - \bar{R}_{xv}^{\text{pn}}(k)}\right]\bar{R}_{xv}^{\text{pn}}(k), \end{aligned} \quad (4.71)$$

$$w_5(k) = -\omega^2 - \frac{1}{2}q^2 + 2\frac{R_v^{\text{ig}}(k)\bar{R}_{xv}^{\text{pn}}(k) - R_v^{\text{pn}}(k)\bar{R}_{xv}^{\text{ig}}(k)}{\bar{R}_{xv}^{\text{ig}}(k) - \bar{R}_{xv}^{\text{pn}}(k)}, \quad (4.72)$$

$$\omega qw_6(k) = -\frac{1}{2}\omega q - \frac{R_v^{\text{ig}}(k) - R_v^{\text{pn}}(k)}{\bar{R}_{xv}^{\text{ig}}(k) - \bar{R}_{xv}^{\text{pn}}(k)} + \frac{\bar{R}_{xv}^{\text{ig}}(k)R_{xv}^{\text{pn}}(k) - \bar{R}_{xv}^{\text{pn}}(k)R_{xv}^{\text{ig}}(k)}{\bar{R}_{xv}^{\text{ig}}(k) - \bar{R}_{xv}^{\text{pn}}(k)}, \quad (4.73)$$

$$-iqw_7(k) = \omega qw_6(k), \quad (4.74)$$

$$-i\omega w_8(k) = \frac{1}{2}\omega^2 + 2\frac{R_{xv}^{\text{ig}}(k) - R_{xv}^{\text{pn}}(k)}{\bar{R}_{xv}^{\text{ig}}(k) - \bar{R}_{xv}^{\text{pn}}(k)}. \quad (4.75)$$

We observe that all the TCFs are expressed in terms of the ratios (4.62), which are extracted from the linearly dependent solutions to the dynamical EOMs in a single copy of the doubled Schwarzschild-AdS₅. In the next section these results are presented explicitly. Finally, it is very important to realise and straightforward to check that all the symmetry relations imposed by the discrete symmetries (see subsection 2 B) are satisfied by (4.60), (4.61), (4.69)-(4.75) automatically. Furthermore, to demonstrate that one does not actually need to solve the bulk EOMs at all.

5. RESULTS FOR THE TCFS

In this section, all the results for the parameters in the effective Lagrangian (2.2) are presented. For completeness and consistency check, we first consider limits in which analytical calculations could be performed, hereby recovering some of the results available in the literature. Next we switch to numerical analysis.

A. Analytical results

• $\mathbf{q} = 0$

When $q = 0$, $SO(3)$ rotational symmetry is recovered, $\tilde{C}_\perp = \tilde{C}_x = \tilde{C}_i$ and the dynamical EOM (4.27) for this component decouples from that of \tilde{C}_t . The analytical results for the basic set of solutions are

$$\begin{aligned}\tilde{C}_t^{\text{ig}}(r, \omega, q = 0) = 0 &\Rightarrow \tilde{C}_t^{\text{ig}(0)}(\omega, q) = \tilde{C}_t^{\text{ig}(2)}(\omega, q) = 0, \\ \tilde{C}_i^{\text{pn}}(r, \omega, q = 0) = 0 &\Rightarrow \tilde{C}_i^{\text{pn}(0)}(\omega, q) = \tilde{C}_i^{\text{pn}(2)}(\omega, q) = 0.\end{aligned}\quad (5.1)$$

$$\tilde{C}_t^{\text{pn}}(r, \omega, q = 0) = 1 - \frac{r_h^2}{r^2} \Rightarrow \tilde{C}_t^{\text{pn}(0)}(\omega, q = 0) = 1, \quad \tilde{C}_t^{\text{pn}(2)}(\omega, q = 0) = -r_h^2. \quad (5.2)$$

The only non-trivial result is related to the spatial component \tilde{C}_i^{ig} , which is however well known [71, 72]:

$$\begin{aligned}\tilde{C}_i^{\text{ig}}(r, \omega, q = 0) &= \left(1 - \frac{r_h^2}{r^2}\right)^{-i\omega/(4r_h)} \left(1 + \frac{r_h^2}{r^2}\right)^{-\omega/(4r_h)} \left(\frac{r_h^2}{r^2}\right)^{(1+i)\omega/(4r_h)} \\ &\times {}_2F_1\left[1 - \frac{(1+i)\omega}{4r_h}, -\frac{(1+i)\omega}{4r_h}, 1 - \frac{i\omega}{2r_h}, \frac{1}{2}\left(1 - \frac{r_h^2}{r^2}\right)\right],\end{aligned}\quad (5.3)$$

where ${}_2F_1$ is a hypergeometric function. Near the AdS boundary,

$$\begin{aligned}\frac{\tilde{C}_i^{\text{ig}(2)}(\omega, q = 0)}{\tilde{C}_i^{\text{ig}(0)}(\omega, q = 0)} &= -r_h^2 \tilde{\omega} \left\{ i + [2\gamma_e - 1 + \log(2r_h^2/L^2)] \tilde{\omega} + \tilde{\omega} \psi \left(-\frac{(1+i)}{2} \tilde{\omega} \right) \right. \\ &\quad \left. + \tilde{\omega} \psi \left(\frac{(1-i)}{2} \tilde{\omega} \right) \right\},\end{aligned}\quad (5.4)$$

where $\tilde{\omega} = \omega/(2r_h) = \omega\beta/(2\pi)$ is introduced for compactness, $\psi(z) = d\Gamma(z)/dz$, and γ_e is the Euler constant. Here we have reinstalled the AdS curvature radius L in the logarithmic term.

Thus, in the limit $q = 0$ we can fix w_1 , w_2 , w_5 and w_8 while the remaining TCFs decouple:

$$\begin{aligned}w_1(q = 0) &= 0, \\ w_2(q = 0) &= 2 \coth(\pi\tilde{\omega}) \text{Im} \left[\frac{\tilde{C}_\perp^{\text{ig}(2)}(\omega, q = 0)}{\tilde{C}_\perp^{\text{ig}(0)}(\omega, q = 0)} \right], \\ w_5(q = 0) &= -2 \frac{\tilde{C}_t^{\text{pn}(2)}(\omega, q = 0)}{\tilde{C}_t^{\text{pn}(0)}(\omega, q = 0)} = 2r_h^2, \\ w_8(q = 0) &= -\frac{1}{2}i\omega - \frac{2}{i\omega} \frac{\tilde{C}_x^{\text{ig}(2)}(\omega, q = 0)}{\tilde{C}_x^{\text{ig}(0)}(\omega, q = 0)}.\end{aligned}\quad (5.5)$$

- $\omega = \mathbf{q}$

In this limit analytical results are available for the transverse mode \tilde{C}_\perp only [73]. The ingoing solution of the dynamical EOM (4.21) is

$$\begin{aligned} \tilde{C}_\perp^{\text{ig}}(r, \omega = q) &= \left(1 - \frac{r_h^2}{r^2}\right)^{-i\omega/(4r_h)} \left(1 + \frac{r_h^2}{r^2}\right)^{\omega/(4r_h)} \\ &\times {}_2F_1\left[1 - \frac{(1+i)\omega}{4r_h}, -\frac{(1+i)\omega}{4r_h}, 1 - \frac{i\omega}{2r_h}, \frac{1}{2} \left(1 - \frac{r_h^2}{r^2}\right)\right]. \end{aligned} \quad (5.6)$$

Near the AdS boundary $r = \infty$,

$$\frac{\tilde{C}_\perp^{\text{ig}(2)}(\omega = q)}{\tilde{C}_\perp^{\text{ig}(0)}(\omega = q)} = r_h^2 \left[1 - \tilde{\omega} + \left(\frac{1+i}{2}\tilde{\omega} - 1\right) \frac{{}_2F_1(2 - (1+i)\tilde{\omega}/2, -(1+i)\tilde{\omega}/2, 1 - i\tilde{\omega}, 1/2)}{{}_2F_1(1 - (1+i)\tilde{\omega}/2, -(1+i)\tilde{\omega}/2, 1 - i\tilde{\omega}, 1/2)}\right]. \quad (5.7)$$

In the absence of analytical solution in the longitudinal sector, only w_2 and the combination $w_8 + i\omega w_9$ can be determined:

$$\begin{aligned} w_2(\omega = q) &= 2 \coth(\pi\tilde{\omega}) \text{Im} \left[\frac{\tilde{C}_\perp^{\text{ig}(2)}(\omega = q)}{\tilde{C}_\perp^{\text{ig}(0)}(\omega = q)} \right], \\ w_8(\omega = q) + i\omega w_9(\omega = q) &= -\frac{2}{i\omega} \frac{\tilde{C}_\perp^{\text{ig}(2)}(\omega = q)}{\tilde{C}_\perp^{\text{ig}(0)}(\omega = q)}. \end{aligned} \quad (5.8)$$

- **The hydrodynamic limit** $\omega \ll \mathbf{T} \sim \mathbf{r}_h, \mathbf{q} \ll \mathbf{T} \sim \mathbf{r}_h$.

In the hydrodynamic limit, the results available in the literature (see [58] and [59]) pertain to the effective Lagrangian (2.2) up to second order in the derivatives of $B_{r\mu}$ and $B_{a\mu}$. Since our formalism is somewhat different from the others, it makes sense to perform a comparison. Hence we have to obtain analytical results accurate up to second order. Naively, one would expect to achieve this accuracy by solving the bulk EOMs also up to second order in the derivatives of $B_{r\mu}$ and $B_{a\mu}$. However, as can be seen from (4.61), (4.70), and (4.71), in fact one has to solve for the ingoing solutions keeping the third order terms in the derivative expansion.

It is convenient to introduce a new radial coordinate u :

$$u = r_h^2/r^2 \implies \tilde{C}_\mu(r, \omega, q) \rightarrow \tilde{C}_\mu(u, \omega, q). \quad (5.9)$$

The ingoing solution for the transverse mode \tilde{C}_\perp is well known in the literature, see e.g. [11]. Up to third order in momenta the solution is

$$\tilde{C}_\perp^{\text{ig}}(u, \omega, q) = (1 - u^2)^{-i\tilde{\omega}/2} \left\{ 1 + i\tilde{\omega} \log(1 + u) + \frac{1}{24} \pi^2 (3\tilde{\omega}^2 - 2\tilde{q}^2) - \frac{1}{4} \tilde{\omega}^2 \log^2 2 \right\}$$

$$\begin{aligned}
& + \frac{1}{2} \tilde{\omega}^2 \log(1-u) \log \frac{2}{1+u} - \frac{1}{4} \log(1+u) [2(\tilde{\omega}^2 - \tilde{q}^2) \log u + \tilde{\omega}^2 \log(1+u)] \\
& + \frac{1}{2} (\tilde{q}^2 - \tilde{\omega}^2) [\text{Li}_2(1-u) + \text{Li}_2(-u)] - \frac{1}{2} \tilde{\omega}^2 \text{Li}_2 \left(\frac{1+u}{2} \right) + \tilde{C}_\perp^{\text{ig}[3]}(u, \omega, q) + \dots \Big\}, \quad (5.10)
\end{aligned}$$

where Li_2 is the Polylogarithm function, and $\tilde{C}_\perp^{\text{ig}[3]}(u, \omega, q)$ is the third order solution, which is too lengthy to be shown here. Near the AdS boundary $u = 0$,

$$\begin{aligned}
\tilde{C}_\perp^{\text{ig}(0)} &= 1, \\
\tilde{C}_\perp^{\text{ig}(2)} &= r_h^2 \left[i\tilde{\omega} - \tilde{q}^2 + \tilde{\omega}^2 - \tilde{\omega}^2 \log 2 + (\tilde{q}^2 - \tilde{\omega}^2) \log(r_h^2/L^2) + \frac{\pi^2}{12} i\tilde{\omega}(2\tilde{\omega}^2 - 3\tilde{q}^2) \right]. \quad (5.11)
\end{aligned}$$

Most of the results about the longitudinal sector available in the literature are based on the on-shell holography, which for this reason cannot be recycled for our study. In the off-shell formalism similar to ours, recently the authors of [58] worked out the hydrodynamic limit of the independent solutions $\{\tilde{C}_t, \tilde{C}_x\}$ (see appendix B there), though up to second order only. We have computed the expansion up to third order⁷:

$$\begin{aligned}
\tilde{C}_t^{\text{ig}}(u, \omega, q) &= (1-u^2)^{1-i\tilde{\omega}/2} \left[\frac{i\tilde{q}}{1+u} + \frac{\tilde{\omega}\tilde{q}}{1-u^2} \left(\log \frac{2}{1+u} + u \log u \right) + \tilde{C}_t^{\text{ig}[3]}(u, \omega, q) + \dots \right], \\
\tilde{C}_x^{\text{ig}}(u, \omega, q) &= (1-u^2)^{-i\tilde{\omega}/2} \left\{ 1 + i\tilde{\omega} \log \frac{1+u}{2} + \frac{\pi^2 \tilde{\omega}^2}{24} - \frac{1}{2} \tilde{\omega}^2 \log \frac{1-u}{2} \log \frac{1+u}{2} \right. \\
&\quad - \frac{1}{4} \tilde{\omega}^2 \log^2 \frac{1+u}{2} - \frac{1}{2} \tilde{\omega}^2 \log u \log(1+u) - \frac{1}{2} \tilde{\omega}^2 \text{Li}_2(1-u) - \frac{1}{2} \tilde{\omega}^2 \text{Li}_2(-u) \\
&\quad \left. - \frac{1}{2} \tilde{\omega}^2 \text{Li}_2 \left(\frac{1+u}{2} \right) + \tilde{C}_x^{\text{ig}[3]}(u, \omega, q) + \dots \right\}, \quad (5.12)
\end{aligned}$$

where the third order solutions $\tilde{C}_t^{\text{ig}[3]}(u, \omega, q)$ and $\tilde{C}_x^{\text{ig}[3]}(u, \omega, q)$ have been worked out by us, but are too lengthy to be presented here. The near AdS boundary data are

$$\begin{aligned}
\tilde{C}_t^{\text{ig}(0)}(\omega, q) &= i\tilde{q} + \tilde{\omega}\tilde{q} \log 2 + \frac{1}{2} i\tilde{q} (-\tilde{\omega}^2 \log^2 2 + 2\tilde{q}^2 \log 2) + \dots, \\
\tilde{C}_t^{\text{ig}(2)}(\omega, q) &= r_h^2 [-i\tilde{q} - \tilde{\omega}\tilde{q} + \tilde{\omega}\tilde{q} \log(r_h^2/L^2)] - \frac{r_h^2}{12} i\tilde{q} [12\tilde{q}^2 + \pi^2 \tilde{\omega}^2 - 12\tilde{\omega}^2 \log 2 \\
&\quad + 6\tilde{\omega}^2 \log^2 2 + 12\tilde{\omega}^2 \log 2 \log(r_h^2/L^2) - 12\tilde{q}^2 \log(2r_h^2/L^2)] + \dots, \\
\tilde{C}_x^{\text{ig}(0)}(\omega, q) &= 1 - i\tilde{\omega} \log 2 - \frac{1}{12} \tilde{\omega}^2 (\pi^2 + 6 \log^2 2) + \frac{1}{12} i\omega \pi^2 (\tilde{\omega}^2 \log 2 - \tilde{q}^2) \\
&\quad + \frac{1}{6} i\tilde{\omega}^3 (\log^3 2 - 3\zeta(3)) + \dots,
\end{aligned}$$

⁷ Our results are somewhat different from [58]. The origin of the difference is in the freedom to arbitrarily select the horizon data.

$$\begin{aligned}\tilde{C}_x^{\text{rig}(2)}(\omega, q) = & r_h^2 [i\tilde{\omega} + \tilde{\omega}^2 - \tilde{\omega}^2 \log(r_h^2/L^2)] + \frac{r_h^2}{12} i\tilde{\omega} [12\tilde{q}^2 + \pi^2 \tilde{\omega}^2 - 12\tilde{\omega}^2 \log 2 \\ & + 6\tilde{\omega}^2 \log^2 2 + 12\tilde{\omega}^2 \log 2 \log(r_h^2/L^2) - 12q^2 \log(2r_h^2/L^2)] + \dots .\end{aligned}\quad (5.13)$$

Here we have kept terms up to third order in momenta.

Next, we present the hydrodynamic limit of the polynomial solution $\{\tilde{C}_t^{\text{pn}}, \tilde{C}_x^{\text{pn}}\}$:

$$\begin{aligned}\tilde{C}_t^{\text{pn}}(u, \omega, q) = & 2(1-u) + 2\tilde{q}^2 \left[u \log u + (1+u) \log \frac{2}{1+u} \right] + \dots , \\ \tilde{C}_x^{\text{pn}}(u, \omega, q) = & -\tilde{\omega} \tilde{q} \left\{ \frac{1}{4} (\pi^2 - 2 \log^2 2) + \log u \log \frac{1+u}{1-u} + \frac{1}{2} \log(1+u) \log \frac{4}{1+u} \right. \\ & \left. - \text{Li}_2 \left(\frac{1-u}{2} \right) + \text{Li}_2(-u) - \text{Li}_2(u) \right\} + \dots .\end{aligned}\quad (5.14)$$

Near the AdS boundary,

$$\begin{aligned}\tilde{C}_t^{\text{pn}(0)}(\omega, q) = & 2 + 2\tilde{q}^2 \log 2 + \dots , \\ \tilde{C}_t^{\text{pn}(2)}(\omega, q) = & r_h^2 [-2 + 2\tilde{q}^2 (\log 2 - 1) + 2\tilde{q}^2 \log(r_h^2/L^2)] + \dots , \\ \tilde{C}_x^{\text{pn}(0)}(\omega, q) = & -\frac{1}{6} \pi^2 \tilde{\omega} \tilde{q} + \dots , \\ \tilde{C}_x^{\text{pn}(2)}(\omega, q) = & r_h^2 [-2\tilde{\omega} \tilde{q} (\log 2 - 1) - 2\tilde{\omega} \tilde{q} \log(r_h^2/L^2)] + \dots .\end{aligned}\quad (5.15)$$

Finally, we are ready to compute the TCFs in (2.2), based on the hydrodynamic expansion for the bulk fields. From the solution in the transverse sector, we obtain

$$\begin{aligned}w_8 = & -r_h - \frac{1}{2} i\omega [\log 2 + \log(r_h^2/L^2)] + \dots , \\ w_9 = & \frac{1}{2} \log(r_h^2/L^2) + \dots , \\ w_2 = & \frac{2r_h^2}{\pi} + \frac{\pi}{4} \omega^2 - \frac{\pi}{8} q^2 + \dots .\end{aligned}\quad (5.16)$$

From the solutions in the longitudinal sector,

$$\begin{aligned}w_1 = & 0 + \mathcal{O}(\lambda^3), \\ w_3 = & \frac{\pi}{8} + \dots , \\ w_4 = & -\frac{\pi}{24} i\omega + \dots , \\ w_5 = & 2r_h^2 - \frac{1}{2} q^2 [2 \log 2 + \log(r_h^2/L^2)] + \dots , \\ w_6 = & -\frac{\log(2r_h^2/L^2)}{2} + \dots ,\end{aligned}$$

$$w_7 = -\frac{1}{2}i\omega \log(2r_h^2/L^2) + \dots \quad (5.17)$$

The TCFs of (2.19) as well as the noise-noise correlator G_0 are expanded as

$$\begin{aligned} \mathcal{D} &= \frac{1}{2r_h} + \mathcal{O}(\lambda^2), & \sigma_e &= r_h + \frac{1}{2}i\omega \log \frac{2r_h^2}{L^2} + \mathcal{O}(\lambda^2), & \sigma_m &= \frac{1}{2} \log \frac{r_h^2}{L^2} + \mathcal{O}(\lambda^1), \\ \Xi &= \frac{2ir_h^2}{\pi} + \mathcal{O}(\lambda^2), & G_0 &= -\frac{2ir_h^2}{\pi}q^2 + \mathcal{O}(\lambda^4), \end{aligned} \quad (5.18)$$

where $\lambda \sim \partial_\mu$ is the bookkeeping parameter for the derivative expansion. Notice that the relaxation time (order ω term) for the diffusion TCF vanishes. This is not in agreement with the results of [18]. We postpone the comparison with [18] to the end of this section.

We now compare our analytical results in the hydrodynamic limit with those of [58, 59]. It is important to keep in mind that the minimal subtraction counter-term $S_{\text{c.t.}}$ introduced in the present work as well as in [58] differs from the one used in [59]. Ref. [58] claimed agreement with [59] on the values of the transport coefficients. Yet, after careful examination of the results of both papers and taking into account differences originating from the different counter-terms, we fail to see a complete agreement. Below, we detail on the comparison.

Comparison with [58]. Ref. [58] focused on the longitudinal sector only. Hence, it does not have any results on w_9 , neither separately on w_2 and w_3 (only the combination $w_2 + q^2 w_3$ was determined). To ease the comparison, the results of [58] are summarised below.

$$\begin{aligned} w_1^{\text{dBHPF}} &= 0 + \mathcal{O}(\lambda^3), \\ w_2^{\text{dBHPF}} + q^2 w_3^{\text{dBHPF}} &= \frac{2\pi^2 T^2 L}{g_A^2} \frac{1}{\pi} + \mathcal{O}(\lambda^3), \\ w_4^{\text{dBHPF}} &= 0 + \mathcal{O}(\lambda^2), \\ w_5^{\text{dBHPF}} &= \frac{2\pi^2 T^2 L}{g_A^2} - \frac{2\pi^2 T^2 L}{g_A^2} \frac{\log 2}{2\pi^2 T^2} q^2 + \mathcal{O}(\lambda^3), \\ w_6^{\text{dBHPF}} &= -\frac{2\pi^2 T^2 L}{g_A^2} \frac{\log 2}{4\pi^2 T^2} + \mathcal{O}(\lambda^1), \\ w_7^{\text{dBHPF}} &= -\frac{2\pi^2 T^2 L}{g_A^2} \frac{\log 2}{4\pi^2 T^2} i\omega + \mathcal{O}(\lambda^2), \\ w_8^{\text{dBHPF}} &= -\frac{2\pi^2 T^2 L}{g_A^2} \frac{1}{2\pi T} - \frac{2\pi^2 T^2 L}{g_A^2} \frac{\log 2}{4\pi^2 T^2} i\omega + \mathcal{O}(\lambda^2), \end{aligned} \quad (5.19)$$

where g_A is the gauge coupling constant which has been set to one in our work. The $\log(r_h/L)$ terms do not appear in [58], because they have been set to zero.

Our results are largely consistent with those of [58] except

- The ω^2 -term in $w_2 + q^2 w_3$;
- The ω -term in w_4 .

The differences can be presumably attributed to the lack of the third order accuracy in the ingoing solutions $\{\tilde{C}_t, \tilde{C}_x\}$ in [58], which is necessary for correct determination of $w_2 + q^2 w_3$ (up to second order) and w_4 (up to first order).

Comparison with [59]. We quote the results of [59]:

$$\begin{aligned}
w_1^{\text{GCL}} &= 0 + \mathcal{O}(\lambda^3), \\
w_2^{\text{GCL}} &= \frac{2\pi}{\beta^2} + \frac{\pi}{4}\omega^2 - \frac{\pi}{8}q^2 + \mathcal{O}(\lambda^3), \\
w_3^{\text{GCL}} &= \frac{\pi}{8} + \mathcal{O}(\lambda^1), \\
w_4^{\text{GCL}} &= -\frac{2\pi}{\beta} - \frac{48G + 7\pi^2}{96\pi}i\omega + \mathcal{O}(\lambda^2), \\
w_5^{\text{GCL}} &= \frac{2\pi^2}{\beta^2} + \left(\frac{1}{2} - \log 2\right)q^2 + \mathcal{O}(\lambda^3), \\
w_6^{\text{GCL}} &= \frac{1 - \log 2}{2} - \frac{\pi}{4} + \mathcal{O}(\lambda^1), \\
w_7^{\text{GCL}} &= \left(\frac{1 - \log 2}{2} + \frac{\pi}{4}\right)i\omega + \mathcal{O}(\lambda^2), \\
w_8^{\text{GCL}} &= -\frac{\pi}{\beta} + \frac{1 - \log 2}{2}i\omega + \mathcal{O}(\lambda^2), \\
w_9^{\text{GCL}} &= -\frac{1}{2} + \mathcal{O}(\lambda^1).
\end{aligned} \tag{5.20}$$

In order to compare the results, we have to account for the difference between the subtraction terms used here and in [59]. In order to represent the results of [59] within the minimal subtraction scheme, some w_i^{GCL} 's in (5.20) have to be shifted:

$$\begin{aligned}
w_5^{\text{GCL}} &\rightarrow w_5^{\text{GCL}} + q^2 [\log(r_h/L) + 1/2], & w_6^{\text{GCL}} &\rightarrow w_6^{\text{GCL}} + \log(r_h/L) + 1/2, \\
w_7^{\text{GCL}} &\rightarrow w_7^{\text{GCL}} + i\omega [\log(r_h/L) + 1/2], & w_8^{\text{GCL}} &\rightarrow w_8^{\text{GCL}} + i\omega [\log(r_h/L) + 1/2], \\
w_9^{\text{GCL}} &\rightarrow w_9^{\text{GCL}} - \log(r_h/L) - 1/2, & \text{others are not changed.}
\end{aligned} \tag{5.21}$$

With the differences in the counter-terms taken into account, our results agree with those of [59] except

- w_4 is completely different. The relevant result in [59] appears to be also in disagreement with [58]. We also notice that w_4^{GCL} does not seem to satisfy the KMS condition (2.12).

- w_6 and w_7 . Both w_6^{GCL} , w_7^{GCL} do not obey the KMS condition (2.11).

We have attempted to trace the origin of these differences. First of all, our approach to solving the bulk dynamics is quite different from that of [59]. Particularly, the horizon limit ($\epsilon \rightarrow 0$) in our formalism is always taken before the hydrodynamic limit ($\partial_\mu \rightarrow 0$). This is in contrast to [59], which performs the hydrodynamic expansion at the level of the dynamical EOMs. These two limits do not always commute. Particularly, it is important to keep the oscillating factors like $e^{i\omega\zeta_1(r)}$ unexpanded.

B. Numerical results at finite ω and q

Except for the couple of special cases of vanishing three-momentum ($q = 0$) and light-like momenta ($\omega = q$), solutions of the ODEs (4.9), (4.10) at finite frequency and momentum are not known analytically. Therefore, in order to provide complete information about the TCFs, we resort to numerical techniques. As has been extensively explained above, we have to solve the dynamical EOMs in a single Schwarzschild-AdS for the ingoing modes and also for the polynomial one, in the longitudinal sector. We solve the equations in the Schwarzschild coordinates and then transform to EF coordinates. Once the solutions are found, we first numerically extract the coefficients of the near boundary expansion and then compute w_i and other TCFs according to (4.60), (4.61), (4.69)-(4.75) and (2.16).

In the bulk model there are two in principle independent length parameters: r_h and the AdS radius L . In the metric (3.1) $L = 1$. For the numerical results to be presented next, we also set $r_h = 1$. There are two consequences of this choice. First, the results do not include the logarithmic branch proportional to $\log(r_h/L)$, though it is not difficult to recover it analytically. Second, r_h becomes a unit of length for all dimension-full quantities such as frequency and momentum. Thus all the results below will be shown for dimensionless $\omega \rightarrow \omega/r_h$ and $q \rightarrow q/r_h$, while we stick to the same notations to avoid introducing new ones.

While the effective Lagrangian (2.2) is parameterised by nine TCFs, the discrete symmetries induce relations (2.8)-(2.12) which leave only four of them independent. Specifically, we have chosen to take w_5 , w_7 , w_8 and w_9 as independent for which the numerical results are presented in Appendix D.

The TCFs that have physical interpretation and hence are more interesting are the ones

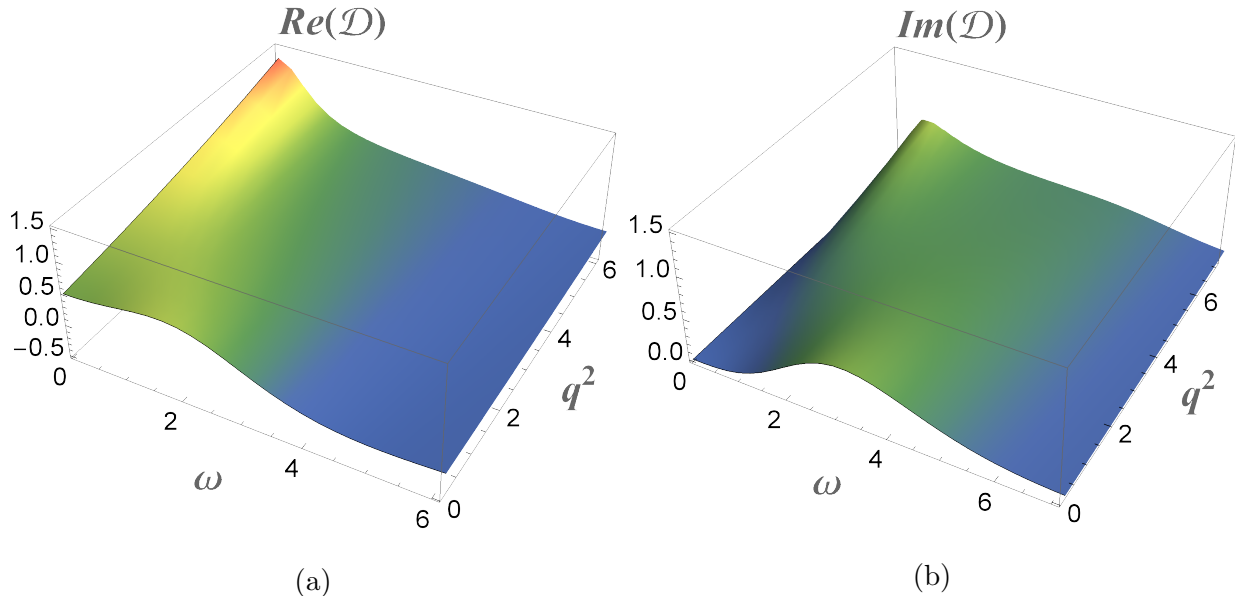


FIG. 2: The ω -, q -dependence of (a) $Re(\mathcal{D}(\omega, q^2))$, (b) $Im(\mathcal{D}(\omega, q^2))$.

parameterising the constitutive relation for the physical current (2.19). Those are the diffusion TCF \mathcal{D} , the electric conductivity σ_e , the magnetic conductivity σ_m , and the thermal force Ξ , whose expressions in terms of w_i are given in (2.16) and (2.20).

The results are summarized in FIGs-2 ,3, 4, 5. At vanishing frequency and momentum both the diffusion constant and electric conductivity are well known: $\mathcal{D}[\omega = q = 0] = 1/2$ [10] and $\sigma_e[\omega = q = 0] = 1$ [73]. When $q = 0$, σ_e is known analytically [71, 72]. Our numerical results are fully consistent with all known analytical results.

Beyond the hydrodynamic limit, both the diffusion TCF \mathcal{D} , the magnetic conductivity σ_m , and Ξ vanish at large frequencies ω . In contrast, σ_e is monotonically increasing function of ω ; particularly $Re(\sigma_e) \sim \omega$ asymptotically. As functions of the three-momentum q , we mostly notice a very mild dependence reflecting quasi-locality. $Re(\Xi)$ scales with q^2 at not too large momentum, hence we plot $Re(\Xi/q^2)$ in FIG. 5.

The TCFs \mathcal{D} , σ_e , σ_m have been originally computed in [18], using the off-shell holography in a single Schwarzschild-AdS₅ geometry. Compared with the results of [18], the present results for the TCFs have different profiles. The origin of the discrepancy is not obvious. We will discuss it in Section 6. Despite the disagreement in the TCFs, the current-current retarded correlators $G_R^{\mu\nu}$ (C.1) are all found to coincide. The equivalence is proven analytically in Appendix C. We have also cross-checked the result numerically.

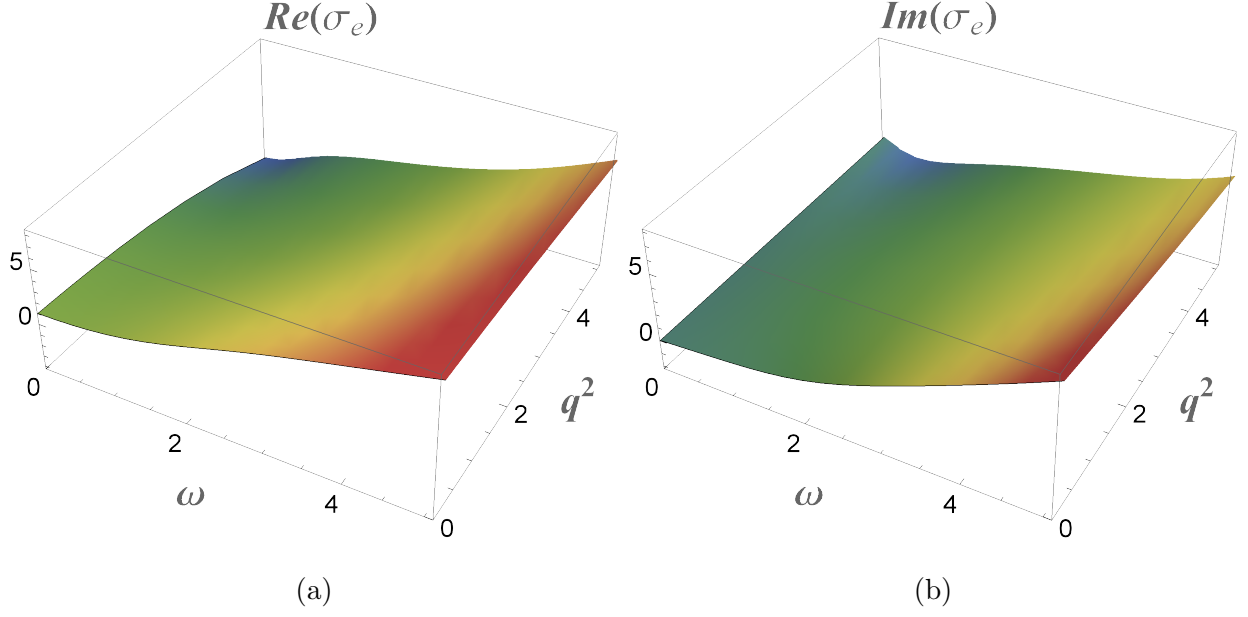


FIG. 3: The ω -, q -dependence of (a) $Re(\sigma_e(\omega, q^2))$, (b) $Im(\sigma_e(\omega, q^2))$.

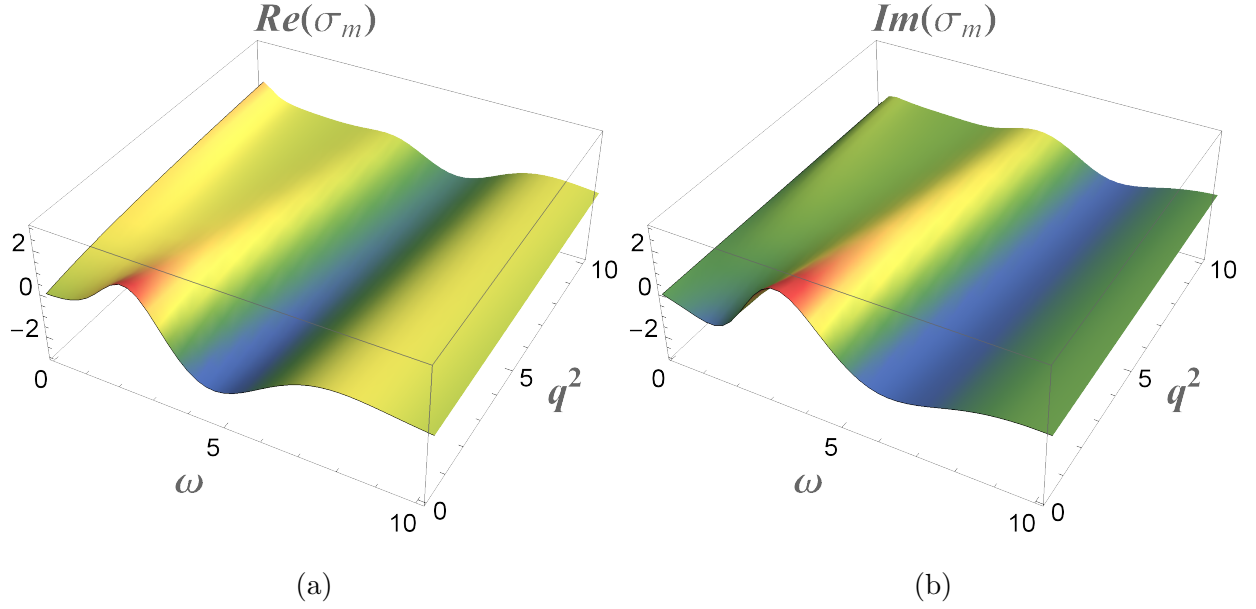


FIG. 4: The ω -, q -dependence of (a) $Re(\sigma_m(\omega, q^2))$, (b) $Im(\sigma_m(\omega, q^2))$.

The noise-noise correlator

Finally, the noise-noise correlator $-iG_0$ is displayed in FIG. 6 as a function of ω and q^2 . In FIG. 7a, we plot the same function, but as 2d slices at fixed representative values of q^2 . Since $-iG_0$ is proportional to q^2 up to sufficiently large momentum, we scale this

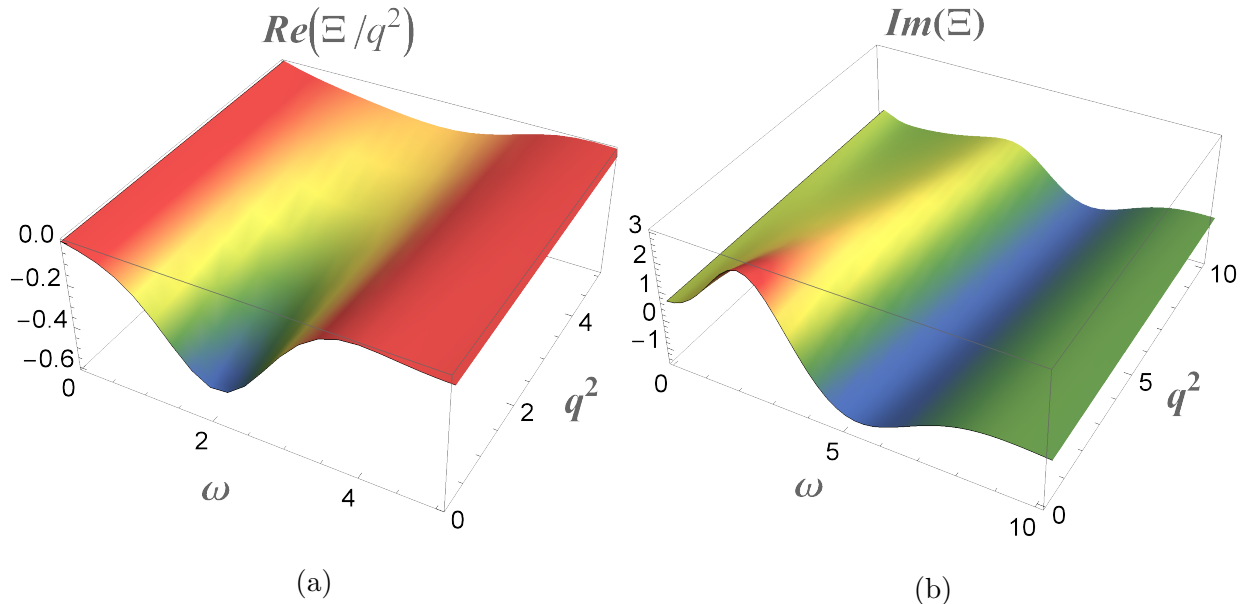


FIG. 5: The ω -, q -dependence of the coefficients (a) $Re(\Xi(\omega, q^2))$ (b) $Im(\Xi(\omega, q^2))$

dependence out in FIGs. 6 and 7a. As is clear from the plots, $-iG_0$ initially oscillates as function of ω but quickly vanishes at large frequencies.

In order to better illustrate the coloured nature of the noise-noise correlator, we perform an inverse Fourier transform of $-iG_0$ with respect to the frequency, thus obtaining the time dependence of the correlator. The analysis is performed for fixed values of momentum q and the results are displayed in FIG.-7b. It might be interesting to additionally perform the inverse Fourier transform in the momentum, so to obtain the full space-time dependence of the correlator. Yet, this turns out to be numerically too expensive and we have decided not to pursue this analysis.

6. SUMMARY AND OUTLOOK

In this work we have further developed the off-shell SK holography. While the core element of the formalism is the geometry proposed in [59], our approach to solving the bulk EOMs is different from that of [59]. When discussing the hydrodynamic expansion, one has to be very careful with the non-commutativity of the hydrodynamic limit vs the near horizon limit. Particularly, in order to reach a certain accuracy in the effective action, EOMs must be expanded to higher orders in the momenta. Our formalism completely avoids this

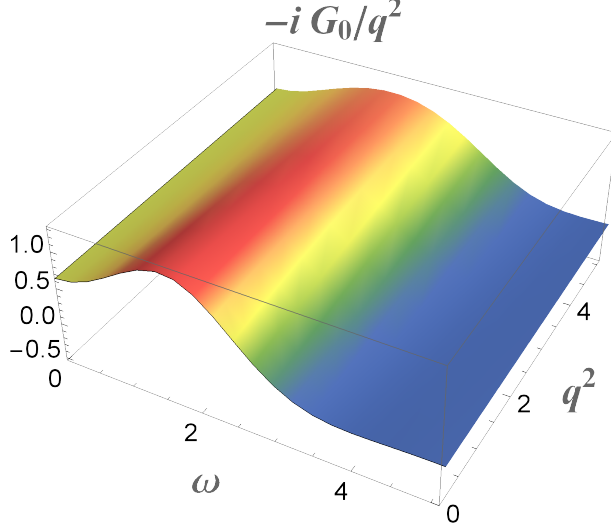


FIG. 6: The ω -, q^2 -dependence of $-iG_0(\omega, q^2)/q^2$

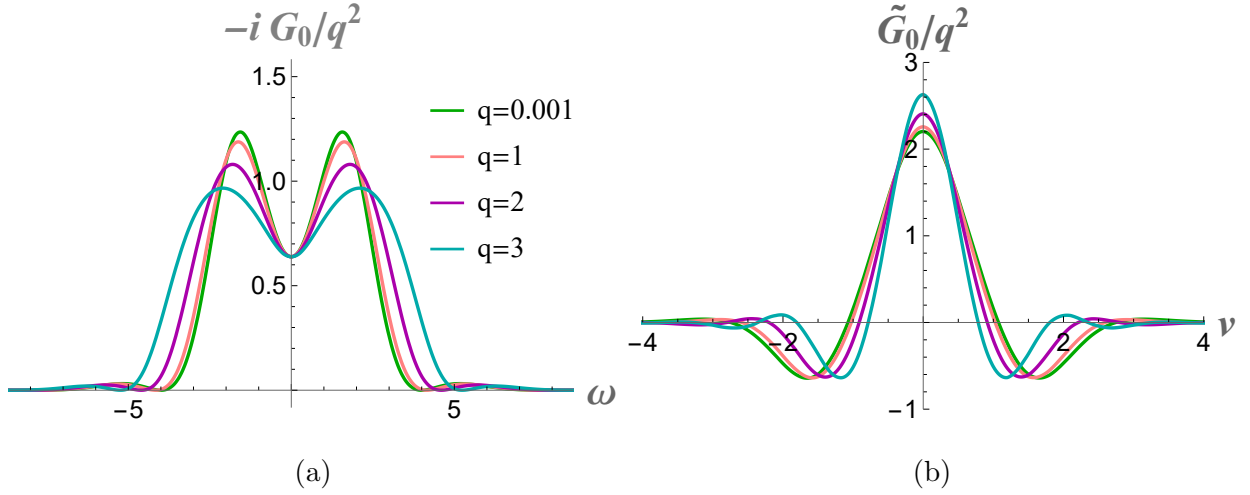


FIG. 7: (a) The ω -dependence of $-iG_0(\omega)/q^2$ at fixed q -slices; (b) The inverse Fourier transform of $-iG_0(\omega)/q^2$ at fixed q -slices.

subtlety since at no place it relies on the hydrodynamic expansion.

Starting from the off-shell SK holography, we have derived the effective action [29] for the charge diffusion and computed all order TCFs ($w_1 \dots w_9$) parameterising it. These TCFs display various types of behaviour as functions of momenta, without any clear pattern. The evolution of $w_1 \dots w_9$ from small momenta (the hydrodynamic limit) to very large momenta can be thought as a flow of the effective action from IR to UV. While we have not analysed it in any detail, the flow corresponds to *integrating in* of the heavy quasi-normal modes. It

would be interesting to better understand this relation. Putting the effective action on-shell, we reproduced the prescription [13] for the retarded two-point current-current correlators.

The constitutive relation (1.3) for the current follows from the off-shell effective action. It is parameterised by four TCFs: the diffusion, electric conductivity, magnetic conductivity, and a thermal force. The latter is a new element emerging from the SK formalism. The thermal force is responsible for fluctuations/noise in the current. Due to linearity of the Maxwell's theory in the bulk, the noise is Gaussian, though coloured (non-local in space-time). We have demonstrated that by explicitly performing the inverse Fourier transform of the noise-noise correlator to the real time.

Our new results for the the diffusion TCF, electric and magnetic conductivities are different from the ones reported earlier in [18], even though they lead to identical two-point retarded correlators. We are not clear about the origin of the disagreement. One possibility is that the off-shell formalism of [18] is not fully correct since it is not based on the SK holography, and might not be derivable from the latter. Alternative possibility is that the off-shell formalism is not unique. Hence TCFs cannot be determined uniquely either. Particularly, they might not be gauge invariant (the present paper and [18] used different sets of gauge fixing conditions). At this stage, we have not investigated this puzzle any further.

The Maxwell's theory in the bulk, even though much more complicated than a free scalar theory, provides a simple Gaussian theory on the boundary. A much more challenging problem would be to consider stochastic neutral flows, which amounts to embedding the fluid/gravity correspondence [9–14] (with dissipations only) into an EFT framework. This problem would require us to further develop the SK holography, particularly addressing the questions of non-Gaussian noise, dynamical horizon, etc.

Another very interesting direction would be to learn about hydrodynamic fluctuations associated with transport induced by chiral anomaly. While some relevant discussion could be found in [32, 74–76], the topic remains largely unexplored. From the perspective of the SK holography, the problem could be addressed within the Maxwell-Chern-Simons theory in the bulk. Stochastic chiral hydrodynamics is expected to be rich with many new phenomena.

Appendix A: The effective action from the basis decomposition

In this appendix we demonstrate how the effective action (2.2) is derived from (3.24). Following the formalism of [18], the bulk gauge fields C_μ can be linearly decomposed in terms of the basic tensor structures built from $B_{r\mu}$ and $B_{a\mu}$,

$$\begin{aligned} C_v &= S_1 B_{rv} + S_2 \partial_k B_{rk} + S_3 B_{av} + S_4 \partial_k B_{ak}, \\ C_i &= V_1 B_{ri} + V_2 \partial_i B_{rv} + V_3 \partial_i \partial_k B_{rk} + V_4 B_{ai} + V_5 \partial_i B_{av} + V_6 \partial_i \partial_k B_{ak}, \end{aligned} \quad (\text{A.1})$$

where the decomposition coefficients (bulk-to-boundary propagators) S_i, V_i are $SO(3)$ scalar functionals of the spacetime derivative operators ∂_μ , and functions of the radial coordinate r :

$$S_i = S_i(r, \partial_v, \vec{\partial}), \quad V_i = V_i(r, \partial_v, \vec{\partial}). \quad (\text{A.2})$$

The boundary conditions for S_i, V_i are translated from those of C_μ ⁸:

$$\begin{aligned} r = \infty_1 : \quad S_1 = V_1 = 1, \quad S_3 = V_4 = \frac{1}{2}, \quad \text{others} = 0, \\ r = \infty_2 : \quad S_1 = V_1 = 1, \quad S_3 = V_4 = -\frac{1}{2}, \quad \text{others} = 0. \end{aligned} \quad (\text{A.3})$$

In Fourier space, $(\partial_v, \vec{\partial}) \rightarrow (-i\omega, i\vec{q})$, these decomposition coefficients become functions of the momenta,

$$S_i(r, \partial_v, \vec{\partial}) \rightarrow S_i(r, \omega, q^2), \quad V_i(r, \partial_v, \vec{\partial}) \rightarrow V_i(r, \omega, q^2), \quad (\text{A.4})$$

With the help of (A.1) the original PDEs (3.16) reduce to a system of linear ODEs. Near $r = \infty_{1,2}$, the decomposition coefficients S_i, V_i can be expanded. Taking into account the boundary conditions (A.3), the expansion takes the form

$$\begin{aligned} S_i(r \rightarrow \infty_1) &= \cdots + \frac{s_{1i}}{r^2} + \cdots, \quad S_i(r \rightarrow \infty_2) = \cdots + \frac{s_{2i}}{r^2} + \cdots, \\ V_i(r \rightarrow \infty_1) &= \cdots + \frac{v_{1i}}{r^2} + \cdots, \quad V_i(r \rightarrow \infty_2) = \cdots + \frac{v_{2i}}{r^2} + \cdots. \end{aligned} \quad (\text{A.5})$$

where the coefficients s_{1i}, v_{1i} and s_{2i}, v_{2i} are respective normalizable modes.

Substituting the decomposition (A.1) into (3.24), the effective Lagrangian in the (r, a) -basis reads

$$\mathcal{L}_{\text{eff}} = -B_{rv} s_{a1} B_{rv} - B_{rv} s_{a2} \partial_k B_{rk} + B_{rk} v_{a1} B_{rk} + B_{rk} v_{a2} \partial_k B_{rv} + B_{rk} v_{a3} \partial_k \partial_l B_{rl}$$

⁸ Our current prescription is somewhat different from that of [18].

$$\begin{aligned}
& + (-B_{rv}s_{a3}B_{av} - B_{av}s_{r1}B_{rv}) + (-B_{rv}s_{a4}\partial_k B_{ak} + B_{ak}v_{r2}\partial_k B_{rv}) \\
& + (-B_{av}s_{r2}\partial_k B_{rk} + B_{rk}v_{a5}\partial_k B_{av}) - B_{av}s_{r3}B_{av} + (-B_{av}s_{r4}\partial_k B_{ak} + B_{ak}v_{r5}\partial_k B_{av}) \\
& + (B_{rk}v_{a4}B_{ak} + B_{ak}v_{r1}B_{rk}) + (B_{rk}v_{a6}\partial_k \partial_l B_{al} + B_{ak}v_{r3}\partial_k \partial_l B_{rl}) + B_{ak}v_{r4}B_{ak} \\
& + B_{ak}v_{r6}\partial_k \partial_l B_{al} + \frac{1}{2}\partial_k B_{ak}\partial_v B_{rv} - \frac{1}{2}B_{av}\partial_v \partial_k B_{rk} + \frac{1}{2}B_{av}\vec{\partial}^2 B_{rv} - \frac{1}{2}B_{ak}\partial_v^2 B_{rk} \\
& + \frac{1}{4}\mathcal{F}_{ajk}\mathcal{F}_{rjk} + B_{av}\partial_v^2 B_{rv}, \tag{A.6}
\end{aligned}$$

Here, the coefficients are represented in the (r, a) -basis:

$$\begin{aligned}
s_{ai} &= s_{1i} - s_{2i}, & s_{ri} &= \frac{1}{2}(s_{1i} + s_{2i}), & i &= 1, 2, 3, 4, \\
v_{ai} &= v_{1i} - v_{2i}, & v_{ri} &= \frac{1}{2}(v_{1i} + v_{2i}), & i &= 1, 2, \dots, 6, \tag{A.7}
\end{aligned}$$

The first line of (A.6) must vanish within the usual (r, a) scheme. Indeed within the holographic representation of the SK contour:

$$s_{a1} = s_{a2} = v_{a1} = v_{a2} = v_{a3} = 0. \tag{A.8}$$

To compare with [29], (A.6) has to be rewritten so that all the a -fields are placed on the left, in all terms, say

$$\int d^4x B_{rv}(x) s_{a3}(\partial_t, \vec{\partial}) B_{av}(x) = \int d^4x B_{av}(x) s_{a3}(-\partial_v, -\vec{\partial}) B_{rv}(x). \tag{A.9}$$

Introducing $w_i = w_i(\partial_v, \vec{\partial})$ as

$$\begin{aligned}
\frac{i}{2}w_1(\partial_v, \vec{\partial}) &= -s_{r3}(\partial_v, \vec{\partial}), \\
\frac{i}{2}w_2(\partial_v, \vec{\partial}) &= v_{r4}(\partial_v, \vec{\partial}), \\
\frac{i}{2}w_3(\partial_v, \vec{\partial}) &= -v_{r6}(\partial_v, \vec{\partial}), \\
iw_4(\partial_v, \vec{\partial}) &= -s_{r4}(\partial_v, \vec{\partial}) - v_{r5}(-\partial_v, -\vec{\partial}), \\
w_5(\partial_v, \vec{\partial}) &= \partial_v^2 + \frac{1}{2}\vec{\partial}^2 - s_{r1}(\partial_v, \vec{\partial}) - s_{a3}(-\partial_v, -\vec{\partial}) \\
w_6(\partial_v, \vec{\partial})\partial_v &= -\frac{1}{2} - s_{r2}(\partial_v, \vec{\partial}) - v_{a5}(-\partial_v, -\vec{\partial}), \\
w_7(\partial_v, \vec{\partial}) &= \frac{1}{2}\partial_v - s_{a4}(-\partial_v, -\vec{\partial}) - v_{r2}(\partial_v, \vec{\partial}) \\
w_8(\partial_v, \vec{\partial})\partial_v &= -\frac{1}{2}\partial_v^2 + v_{a4}(-\partial_v, -\vec{\partial}) + v_{r1}(\partial_v, \vec{\partial}) + [v_{a6}(-\partial_v, -\vec{\partial}) + v_{r3}(\partial_v, \vec{\partial})] \vec{\partial}^2, \\
w_9(\partial_v, \vec{\partial}) &= \frac{1}{2} + v_{a6}(-\partial_v, -\vec{\partial}) + v_{r3}(\partial_v, \vec{\partial}), \tag{A.10}
\end{aligned}$$

the effective Lagrangian (A.6) is cast into (2.2), consistently with [29].

Appendix B: Validating (4.16)

In subsection 4 B, we derived the discontinuity relation (4.16). Our goal here is to verify this condition by computing both left-hand side (LHS) and right-hand side (RHS) of (4.16), starting from the solutions constructed in the subsections 4 C and 4 D.

The RHS of (4.16) is proportional to $\nabla_M F^{Mr}$. Recall that in general, $\nabla_M F^{Mr}$ has a very simple dependence on r , see (3.18). In (3.18) the values of \mathcal{C}^{up} and \mathcal{C}^{dw} should be determined from the solutions established in subsections 4 C and 4 D. As has been emphasised towards the end of subsection 4 C, among the four linearly independent solutions in the longitudinal sector, only the polynomial solution $\{C_v^{\text{pn}}, C_x^{\text{pn}}\}$ does not automatically satisfy the constraint equation (4.8). Hence $\mathcal{C}^{\text{up, dw}}$ must be proportional to the coefficients $n_{\parallel}^{\text{up, dw}}$ multiplying the polynomial solutions. More precisely, by taking the near horizon limit of (3.18), we have

$$\mathcal{C}^{\text{up}}(k) = i\omega r_h^3 \tilde{C}_t^{\text{pn}h} n_{\parallel}^{\text{up}}, \quad \mathcal{C}^{\text{dw}}(k) = i\omega r_h^3 \tilde{C}_t^{\text{pn}h} n_{\parallel}^{\text{dw}}. \quad (\text{B.1})$$

Thus the RHS of (4.16) reads

$$\begin{aligned} \lim_{\Delta \rightarrow 0} \int_{r_- - \Delta}^{r_+ + \Delta} dr \frac{\nabla_M F^{Mr}}{f(r)} &= \frac{\mathcal{C}^{\text{dw}}(k)}{i\omega r_h^3} e^{i\omega \zeta_1(r_h - \epsilon)} - \frac{\mathcal{C}^{\text{up}}(k)}{i\omega r_h^3} e^{i\omega \zeta_2(r_h - \epsilon)} \\ &= \tilde{C}_t^{\text{pn}h} \left[n_{\parallel}^{\text{dw}} e^{i\omega \zeta_1(r_h - \epsilon)} - n_{\parallel}^{\text{up}} e^{i\omega \zeta_2(r_h - \epsilon)} \right]. \end{aligned} \quad (\text{B.2})$$

Based on the solutions found in 4 C and 4 D, the discontinuity of $\partial_r C_v$ is

$$\begin{aligned} \partial_r C_v(r_+) - \partial_r C_v(r_-) &= n_{\parallel}^{\text{up}} \partial_r C_v^{\text{pn}} \Big|_{r=r_+} - n_{\parallel}^{\text{dw}} \partial_r C_v^{\text{pn}} \Big|_{r=r_-} \\ &= \frac{i\omega}{f(r)} n_{\parallel}^{\text{up}} C_v^{\text{pn}}(r) \Big|_{r=r_+} - \frac{i\omega}{f(r)} n_{\parallel}^{\text{dw}} C_v^{\text{pn}}(r) \Big|_{r=r_-} \\ &\quad + \tilde{C}_t^{\text{pn}h} n_{\parallel}^{\text{up}} e^{i\omega \zeta_2(r_h - \epsilon)} - \tilde{C}_t^{\text{pn}h} n_{\parallel}^{\text{dw}} e^{i\omega \zeta_1(r_h - \epsilon)} \end{aligned} \quad (\text{B.3})$$

While C_v is continuous across the cutting slice, $C_r = -C_v/f(r)$ has a jump:

$$\frac{C_v(r)}{f(r)} \Big|_{r=r_+} - \frac{C_v(r)}{f(r)} \Big|_{r=r_-} = \frac{n_{\parallel}^{\text{up}}}{f(r)} C_v^{\text{pn}}(r) \Big|_{r=r_+} - \frac{n_{\parallel}^{\text{dw}}}{f(r)} C_v^{\text{pn}}(r) \Big|_{r=r_-}. \quad (\text{B.4})$$

So, the LHS of (4.16) is computed as

$$\begin{aligned} F^{rv}(r_+) - F^{rv}(r_-) &= \left[\frac{i\omega}{f(r)} - \partial_r \right] C_v \Big|_{r=r_+} - \left[\frac{i\omega}{f(r)} - \partial_r \right] C_v \Big|_{r=r_-} \\ &= \tilde{C}_t^{\text{pn}h} n_{\parallel}^{\text{dw}} e^{i\omega \zeta_1(r_h - \epsilon)} - \tilde{C}_t^{\text{pn}h} n_{\parallel}^{\text{up}} e^{i\omega \zeta_2(r_h - \epsilon)} \end{aligned} \quad (\text{B.5})$$

which is exactly the same as (B.2).

Appendix C: Son-Starinets prescription for retarded correlators revisited

At the early days of the fluid-gravity correspondence, Son and Starinets [13] proposed a prescription for computing Minkowski-space retarded correlators. The prescription is formulated entirely within a single copy of the doubled BH-AdS, and does not rely on SK holography. Yet, a proper derivation of the prescription from the SK holography is missing, and in this appendix we provide one. While there have been earlier works in this direction, particularly [50], which considered SK matrix propagator for a scalar field starting from an eternal black hole in AdS space [70], the SK geometry of [59] adopted here is different. Furthermore, we are not aware of any derivation for the $U(1)$ field available in the literature.

The prescription of [13] relates the retarded correlators to the ingoing solution in a single BH AdS. Starting from the SK holography, we can reproduce the result by taking a few alternative paths. First, the correlators could be obtained from the off-shell effective Lagrangian (2.2) by integrating out the dynamical fields φ_r and φ_a (2.5). The result is the boundary generating functional $W[\mathcal{A}_{a\mu}, \mathcal{A}_{r\mu}]$ of the external fields only, from which the correlators could be read off straightforwardly. For the Lagrangian quadratic in the dynamical fields, like (2.2), integrating out φ_r and φ_a could be done by imposing their classical EOMs. On the bulk side, this corresponds to imposing the constraint equation. Putting the solutions (4.47) on-shell is equivalent to setting $n_{\parallel}^{\text{up}} = n_{\parallel}^{\text{dw}} = 0$, which via (4.51) and (4.52) yields classical solutions for φ_r and φ_a .

Alternatively, we could start with the constitutive relation (2.15), and use the continuity equation, which lead to the retarded current-current correlators expressed in terms of the TCFs [18]:

$$\begin{aligned} G_R^{\perp\perp} &= i\omega\sigma_e + q^2\sigma_m, & G_R^{vv} &= \frac{q^2\sigma_e}{-i\omega + q^2\mathcal{D}}, & G_R^{vx} &= \frac{\omega q\sigma_e}{-i\omega + q^2\mathcal{D}}, \\ G_R^{xx} &= \frac{\omega^2\sigma_e}{-i\omega + q^2\mathcal{D}}. \end{aligned} \tag{C.1}$$

These expressions could be algebraically traced back to the ingoing solution in a single copy of BH-AdS.

Yet, we believe the most illuminating derivation is to reconsider the problem from the very beginning, starting within the on-shell SK holography, which offers a possibility to work directly with gauge invariant fields

$$E_{\perp} = \partial_{\perp}C_v - \partial_v C_{\perp}, \quad E_x = \partial_x C_v - \partial_v C_x, \tag{C.2}$$

EOMs for the bulk electric fields E_\perp and E_x are

$$\begin{aligned} \partial_r [rf(r)\partial_r E_\perp] - 2i\omega r \partial_r E_\perp - i\omega E_\perp - q^2 r^{-1} E_\perp &= 0, \\ \partial_r \left[\frac{rf(r)}{\omega^2 - r^{-2}f(r)q^2} \partial_r E_x \right] - \frac{2i\omega r}{\omega^2 - r^{-2}f(r)q^2} \partial_r E_x + \partial_r \left[\frac{-i\omega r}{\omega^2 - r^{-2}f(r)q^2} \right] E_x \\ - \frac{r^{-1}q^2}{\omega^2 - r^{-2}f(r)q^2} E_x &= 0. \end{aligned} \quad (\text{C.3})$$

In the equation for E_x , there is a singularity at $r = r_h(1 - \omega^2/q^2)^{-1/4}$ for space-like momenta, which is however integrable [73].

The on-shell bulk action (3.5) reads

$$\begin{aligned} S_0 = & -\frac{1}{2} \int \frac{d\omega dq}{(2\pi)^2} \left\{ \frac{r}{i\omega} E_\perp(r, -k) E_\perp(r, k) + \frac{rf(r)}{\omega^2} E_\perp(r, -k) \partial_r E_\perp(r, k) \right. \\ & \left. - \frac{i\omega r}{\omega^2 - r^{-2}f(r)q^2} E_x(r, -k) E_x(r, k) + \frac{rf(r)}{\omega^2 - r^{-2}f(r)q^2} E_x(r, -k) \partial_r E_x(r, k) \right\} \Big|_{r=\infty_1} \\ & + \frac{1}{2} \int \frac{d\omega dq}{(2\pi)^2} \left\{ \frac{r}{i\omega} E_\perp(r, -k) E_\perp(r, k) + \frac{rf(r)}{\omega^2} E_\perp(r, -k) \partial_r E_\perp(r, k) \right. \\ & \left. - \frac{i\omega r}{\omega^2 - r^{-2}f(r)q^2} E_x(r, -k) E_x(r, k) + \frac{rf(r)}{\omega^2 - r^{-2}f(r)q^2} E_x(r, -k) \partial_r E_x(r, k) \right\} \Big|_{r=\infty_2}. \end{aligned} \quad (\text{C.4})$$

Near each AdS boundary, $r \rightarrow \infty_s$ with $s = (1, 2)$, the bulk electric fields E_\perp and E_x behave as

$$\begin{aligned} E_{s,\perp}(r, k) &\xrightarrow{r \rightarrow \infty_s} E_{s,\perp}^{(0)}(k) - \frac{i\omega}{r} E_{s,\perp}^{(0)}(k) + \frac{1}{2}(\omega^2 - q^2) E_{s,\perp}^{(0)}(k) \frac{\log r}{r^2} + \frac{E_{s,\perp}^{(2)}(k)}{r^2} + \dots, \\ E_{s,x}(r, k) &\xrightarrow{r \rightarrow \infty_s} E_{s,x}^{(0)}(k) - \frac{i\omega}{r} E_{s,x}^{(0)}(k) + \frac{1}{2}(\omega^2 - q^2) E_{s,x}^{(0)}(k) \frac{\log r}{r^2} + \frac{E_{s,x}^{(2)}(k)}{r^2} + \dots, \end{aligned} \quad (\text{C.5})$$

Then, the generating functional of the boundary theory (i.e., the on-shell bulk action) becomes

$$W[\mathcal{A}_{a\mu}, \mathcal{A}_{r\mu}] = S_0 + S_{\text{c.t.}} = \int \frac{d\omega dq}{(2\pi)^2} \mathcal{L}_{\text{eff}}^{\text{os}}[\mathcal{F}_{alv}, \mathcal{F}_{rlv}], \quad (\text{C.6})$$

where

$$\begin{aligned} \mathcal{L}_{\text{eff}}^{\text{os}} = & \frac{1}{\omega^2} \left[\mathcal{F}_{a\perp v}(-k) E_{r\perp}^{(2)}(k) + \mathcal{F}_{r\perp v}(-k) E_{a\perp}^{(2)}(k) \right] \\ & + \frac{1}{\omega^2 - q^2} \left[\mathcal{F}_{axv}(-k) E_{rx}^{(2)}(k) + \mathcal{F}_{rxv}(-k) E_{ax}^{(2)}(k) \right] \\ & + \frac{1}{2} \mathcal{F}_{a\perp v}(-k) \mathcal{F}_{r\perp v}(-k) + \frac{1}{2} \mathcal{F}_{ax\perp}(-k) \mathcal{F}_{rx\perp}(k) + \frac{\omega^2 + q^2}{2(\omega^2 - q^2)} \mathcal{F}_{axv}(-k) \mathcal{F}_{rxv}(k). \end{aligned} \quad (\text{C.7})$$

The EOMs (C.3) are solved similarly to the transverse sector C_\perp in Section 4. The piecewise solutions will be glued under matching conditions derived in subsection 4 B (imposing the constraint equation $\nabla_M F^{Mr} = 0$)

$$E_i(r_+) = E_i(r_-), \quad f(r_h - \epsilon) [\partial_r E_i(r_+) - \partial_r E_i(r_-)] = 0, \quad i = \perp, x. \quad (\text{C.8})$$

Near the boundaries

$$E_i(r \rightarrow \infty_1) = \mathcal{F}_{1iv}, \quad E_i(r \rightarrow \infty_2) = \mathcal{F}_{2iv}, \quad i = \perp, x, \quad (\text{C.9})$$

Over the entire contour of FIG. 1, the solutions for E_\perp and E_x are

$$\begin{aligned} E_\perp^{\text{up}}(r, \omega, q) &= l_\perp E_\perp^{\text{ig}}(r, \omega, q) + m_\perp E_\perp^{\text{ig}}(r, -\omega, q) e^{2i\omega\zeta_2(r)}, & r \in [r_h - \epsilon, \infty_2), \\ E_\perp^{\text{dw}}(r, \omega, q) &= l_\perp E_\perp^{\text{ig}}(r, \omega, q) + m_\perp e^{-\beta\omega} E_\perp^{\text{ig}}(r, -\omega, q) e^{2i\omega\zeta_1(r)}, & r \in [r_h - \epsilon, \infty_1), \end{aligned} \quad (\text{C.10})$$

$$\begin{aligned} E_x^{\text{up}}(r, \omega, q) &= l_x E_x^{\text{ig}}(r, \omega, q) + m_x E_x^{\text{ig}}(r, -\omega, q) e^{2i\omega\zeta_2(r)}, & r \in [r_h - \epsilon, \infty_2), \\ E_x^{\text{dw}}(r, \omega, q) &= l_x E_x^{\text{ig}}(r, \omega, q) + m_x e^{-\beta\omega} E_x^{\text{ig}}(r, -\omega, q) e^{2i\omega\zeta_1(r)}, & r \in [r_h - \epsilon, \infty_1), \end{aligned} \quad (\text{C.11})$$

where the superposition coefficients l_\perp , m_\perp , l_x and m_x are

$$\begin{aligned} l_\perp &= \frac{\mathcal{F}_{r\perp v}(k)}{E_\perp^{\text{ig}(0)}(k)} + \frac{1}{2} \coth \frac{\beta\omega}{2} \frac{\mathcal{F}_{a\perp v}(k)}{E_\perp^{\text{ig}(0)}(k)}, & m_\perp &= -\frac{\mathcal{F}_{a\perp v}(k)}{(1 - e^{-\beta\omega}) E_\perp^{\text{ig}(0)}(\bar{k})}, \\ l_x &= \frac{\mathcal{F}_{rxv}(k)}{E_x^{\text{ig}(0)}(k)} + \frac{1}{2} \coth \frac{\beta\omega}{2} \frac{\mathcal{F}_{axv}(k)}{E_x^{\text{ig}(0)}(k)}, & m_x &= -\frac{\mathcal{F}_{axv}(k)}{(1 - e^{-\beta\omega}) E_x^{\text{ig}(0)}(\bar{k})}, \end{aligned} \quad (\text{C.12})$$

The near-boundary expansion of the ingoing solutions is

$$\begin{aligned} E_\perp^{\text{ig}}(r, k) &\xrightarrow{r \rightarrow \infty} E_\perp^{\text{ig}(0)}(k) - \frac{i\omega E_\perp^{\text{ig}(0)}(k)}{r} + \frac{1}{2}(\omega^2 - q^2) E_\perp^{\text{ig}(0)}(k) \frac{\log r}{r} + \frac{E_\perp^{\text{ig}(2)}(k)}{r^2} + \dots, \\ E_x^{\text{ig}}(r, k) &\xrightarrow{r \rightarrow \infty} E_x^{\text{ig}(0)}(k) - \frac{i\omega E_x^{\text{ig}(0)}(k)}{r} + \frac{1}{2}(\omega^2 - q^2) E_x^{\text{ig}(0)}(k) \frac{\log r}{r} + \frac{E_x^{\text{ig}(2)}(k)}{r^2} + \dots. \end{aligned} \quad (\text{C.13})$$

Substituting the superposition coefficients and representing the result in the (r, a) -basis, the field's normalisable modes are

$$\begin{aligned} E_{a\perp}^{(2)}(k) &= \frac{E_\perp^{\text{ig}(2)}(\bar{k})}{E_\perp^{\text{ig}(0)}(\bar{k})} \mathcal{F}_{a\perp v}(k), \\ E_{r\perp}^{(2)}(k) &= \frac{1}{2} \coth \frac{\beta\omega}{2} \left[\frac{E_\perp^{\text{ig}(2)}(k)}{E_\perp^{\text{ig}(0)}(k)} - \frac{E_\perp^{\text{ig}(2)}(\bar{k})}{E_\perp^{\text{ig}(0)}(\bar{k})} \right] \mathcal{F}_{a\perp v}(k) + \frac{E_\perp^{\text{ig}(2)}(k)}{E_\perp^{\text{ig}(0)}(k)} \mathcal{F}_{r\perp v}(k), \\ E_{ax}^{(2)}(k) &= \frac{E_x^{\text{ig}(2)}(\bar{k})}{E_x^{\text{ig}(0)}(\bar{k})} \mathcal{F}_{axv}(k), \end{aligned}$$

$$E_{rx}^{(2)}(k) = \frac{1}{2} \coth \frac{\beta\omega}{2} \left[\frac{E_x^{\text{ig}(2)}(k)}{E_x^{\text{ig}(0)}(k)} - \frac{E_x^{\text{ig}(2)}(\bar{k})}{E_x^{\text{ig}(0)}(\bar{k})} \right] \mathcal{F}_{axv}(k) + \frac{E_x^{\text{ig}(2)}(k)}{E_x^{\text{ig}(0)}(k)} \mathcal{F}_{rxv}(k). \quad (\text{C.14})$$

Finally, (C.7) reads

$$\begin{aligned} \mathcal{L}_{\text{eff}}^{\text{os}} = & \frac{1}{\omega^2} \mathcal{F}_{a\perp v}(-k) \frac{1}{2} \coth \frac{\beta\omega}{2} \left[\frac{E_{\perp}^{\text{ig}(2)}(k)}{E_{\perp}^{\text{ig}(0)}(k)} - \frac{E_{\perp}^{\text{ig}(2)}(\bar{k})}{E_{\perp}^{\text{ig}(0)}(\bar{k})} \right] \mathcal{F}_{a\perp v}(k) \\ & + \frac{1}{\omega^2} \mathcal{F}_{a\perp v}(-k) \left[\frac{2E_{\perp}^{\text{ig}(2)}(k)}{E_{\perp}^{\text{ig}(0)}(k)} + \frac{1}{2}\omega^2 + \frac{1}{2}q^2 \right] \mathcal{F}_{r\perp v}(k) \\ & + \frac{1}{\omega^2 - q^2} \mathcal{F}_{axv}(-k) \frac{1}{2} \coth \frac{\beta\omega}{2} \left[\frac{E_x^{\text{ig}(2)}(k)}{E_x^{\text{ig}(0)}(k)} - \frac{E_x^{\text{ig}(2)}(\bar{k})}{E_x^{\text{ig}(0)}(\bar{k})} \right] \mathcal{F}_{axv}(k) \\ & + \frac{1}{\omega^2 - q^2} \mathcal{F}_{axv}(-k) \left[\frac{2E_x^{\text{ig}(2)}(k)}{E_x^{\text{ig}(0)}(k)} + \frac{1}{2}\omega^2 + \frac{1}{2}q^2 \right] \mathcal{F}_{rxv}(k). \end{aligned} \quad (\text{C.15})$$

From the generating functional W , it is straightforward to read off all two-point correlation functions:

$$\begin{aligned} G_R^{\perp\perp} &= \Pi^T(k), & G_S^{\perp\perp} &= G^T(k), \\ G_R^{vv} &= \frac{q^2}{\omega^2 - q^2} \Pi^L(k), & G_R^{vx} &= \frac{\omega q}{\omega^2 - q^2} \Pi^L(k), & G_R^{xx} &= \frac{\omega^2}{\omega^2 - q^2} \Pi^L(k), \\ G_S^{vv} &= \frac{q^2}{\omega^2 - q^2} G^L(k), & G_S^{vx} &= \frac{\omega q}{\omega^2 - q^2} G^L(k), & G_S^{xx} &= \frac{\omega^2}{\omega^2 - q^2} G^L(k), \end{aligned} \quad (\text{C.16})$$

where

$$\begin{aligned} \Pi^T(k) &= \frac{2E_{\perp}^{\text{ig}(2)}(k)}{E_{\perp}^{\text{ig}(0)}(k)} + \frac{1}{2}\omega^2 + \frac{1}{2}q^2, & \Pi^L(\omega, q) &= \frac{2E_x^{\text{ig}(2)}(k)}{E_x^{\text{ig}(0)}(k)} + \frac{1}{2}\omega^2 + \frac{1}{2}q^2, \\ G^T(k) &= \frac{1}{2} \coth \frac{\beta\omega}{2} \left[\frac{E_{\perp}^{\text{ig}(2)}(k)}{E_{\perp}^{\text{ig}(0)}(k)} - \frac{E_{\perp}^{\text{ig}(2)}(\bar{k})}{E_{\perp}^{\text{ig}(0)}(\bar{k})} \right], \\ G^L(k) &= \frac{1}{2} \coth \frac{\beta\omega}{2} \left[\frac{E_x^{\text{ig}(2)}(k)}{E_x^{\text{ig}(0)}(k)} - \frac{E_x^{\text{ig}(2)}(\bar{k})}{E_x^{\text{ig}(0)}(\bar{k})} \right]. \end{aligned} \quad (\text{C.17})$$

From the EOMs (C.3), it is clear that E_{\perp}, E_x are functions of q^2 . So, (C.17) satisfy the FDRs:

$$G^T(\omega, q) = \frac{1}{2} \coth \frac{\beta\omega}{2} \text{Im} [\Pi^T(\omega, q)], \quad G^L(\omega, q) = \frac{1}{2} \coth \frac{\beta\omega}{2} \text{Im} [\Pi^L(\omega, q)]. \quad (\text{C.18})$$

We have reproduced the prescription of [13] for the retarded correlators. A couple of comments are in order. The above derivations have not imposed any KMS-type conditions, rather they follow from the SK holography. The original prescription of [13] correctly but

a-priori unjustifiably ignores the horizon contribution to the on-shell action. From our derivation it is clear that only two AdS boundaries contribute to the boundary generating functional.

Appendix D: Numerical results for w_5, w_7, w_8, w_9

The results for ω -, q -dependence of the coefficients w_5 , w_7 , w_8 and w_9 are displayed as 3D plots in FIGs-8, 9, 10, 11 respectively. The real part of w_5 and imaginary parts of w_7 and w_8 have power like behaviour at large values of ω and q . It is thus more illuminative to have these asymptotic behaviours subtracted. Hence in FIGs-8a, 9a, 10b, we plot $Re(\bar{w}_5) = Re(w_5 + \omega^2 + q^2/2)$, $Im(\bar{w}_7) = Im(w_7 + i\omega/2)$, $Im(\bar{w}_8) = Im(w_8 - i\omega/2)$.

There is no clear universal pattern in the functional dependencies of these TCFs. They display different asymptotic behaviours at large momenta. For example, imaginary part of w_5 develops a growing ridge-like structure in the $\omega \simeq q$ region; imaginary parts of both \bar{w}_7 and \bar{w}_8 display a decreasing ridge-like behaviour also in the vicinity of $\omega \simeq q$ domain. For larger values of frequency (not shown in the plots), the amplitudes of all the TCFs (w_5, w_7, w_8, w_9) seem to keep on growing. Each individual coefficient w_i does not seem to have a clear physical interpretation and this is the reason in the main part of the text we rather focus on the diffusion TCF \mathcal{D} and conductivities σ_e and σ_m only.

It is important to notice that some of the TCs w_i vanish in the hydro limit. Yet all of the TCFs are non-zero at finite momenta and contribute non-trivially to the effective action. In a sense this constitutes an evolution of the effective action from IR (hydro regime) to UV (all order/large momenta regime).

ACKNOWLEDGEMENTS

We would like to thank Song He, Shu Lin and Tianchun Zhou for useful discussions. YB was supported by the Natural Science Foundation of China (NSFC) under the grant No.11705037. TD and ML were supported by the Israeli Science Foundation (ISF) grant #1635/16 and the BSF grants #2012124 and #2014707. TD was supported in part by the JRG Program at the APCTP through the Science and Technology Promotion Fund and Lottery Fund of the Korean Government and also by the Korean Local Governments —

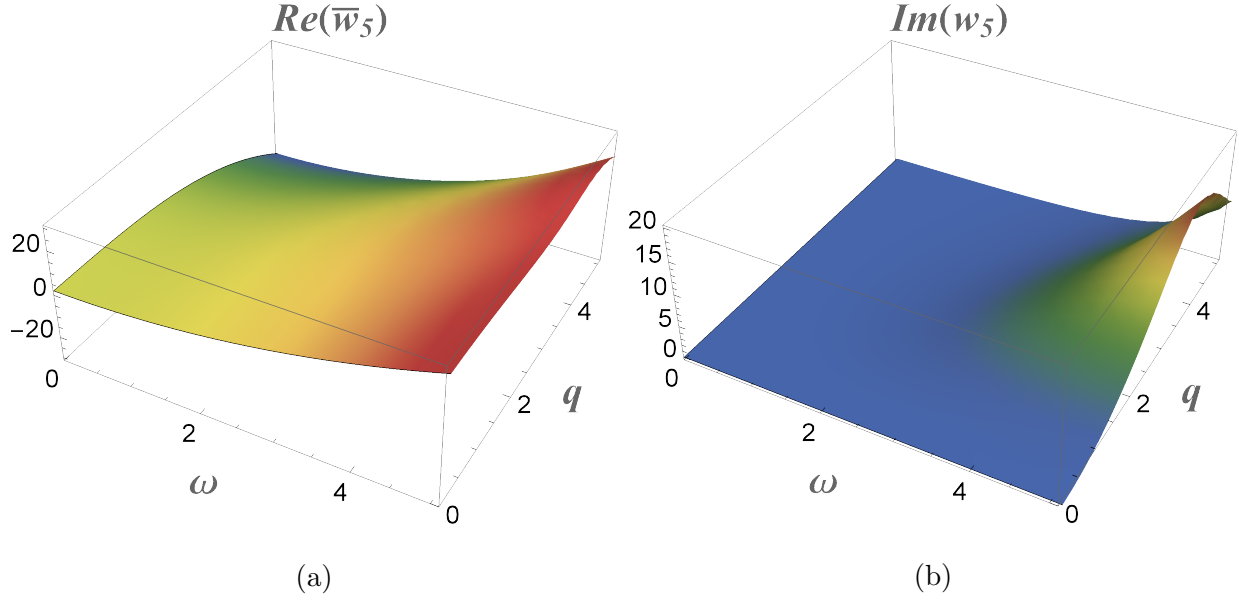


FIG. 8: Plots for ω -, q -dependence of the coefficients (a) $Re(\bar{w}_5(\omega, q))$, (b) $Im(w_5(\omega, q))$.

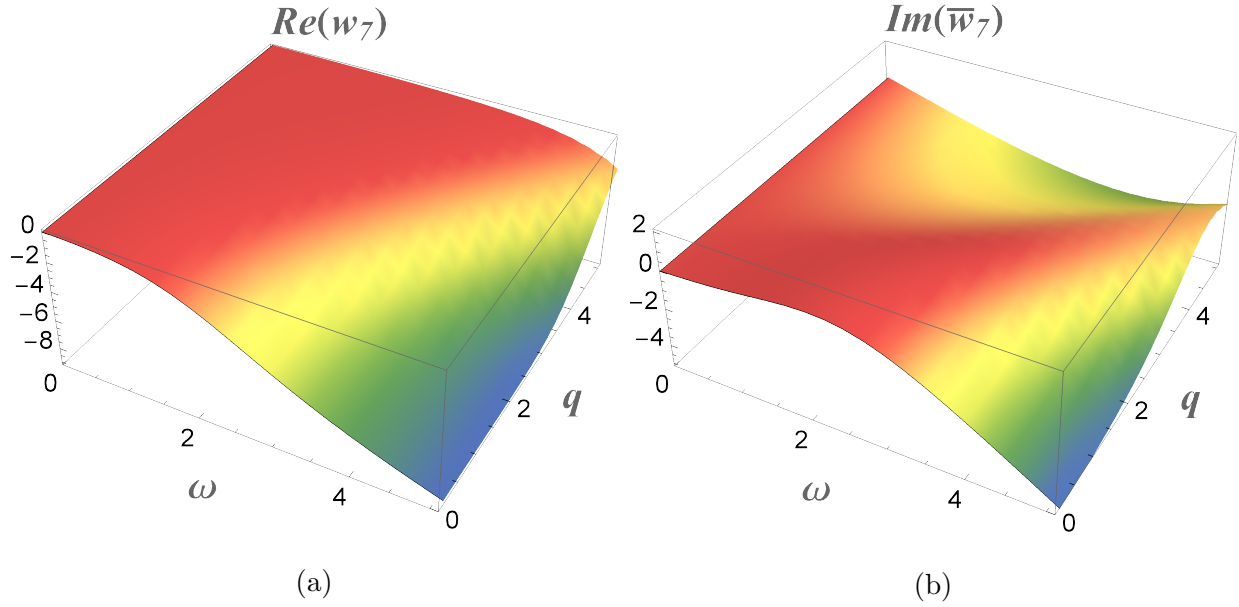


FIG. 9: Plots for ω -, q -dependence of the coefficients (a) $Re(w_7(\omega, q))$, (b) $Im(\bar{w}_7(\omega, q))$.

Gyeongsangbuk-do Province and Pohang City.

[1] L. Landau and E. Lifshitz, *Fluid Mechanics*. No. v. 6. Elsevier Science, 2013.

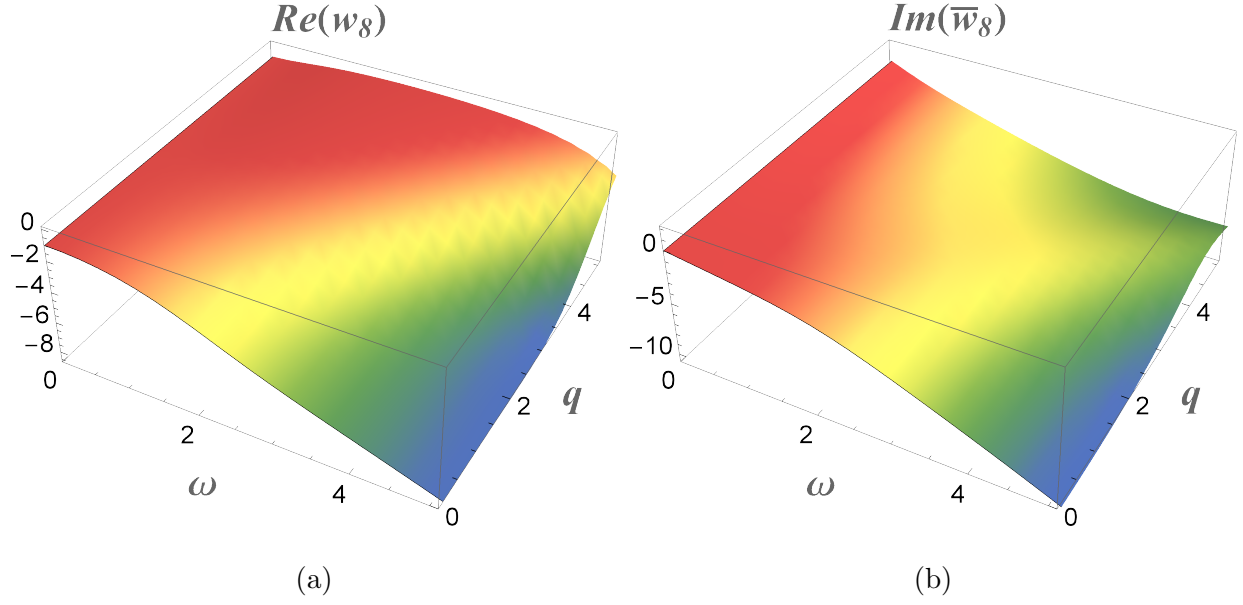


FIG. 10: Plots for ω -, q -dependence of the coefficients (a) $Re(w_8(\omega, q))$, (b) $Im(\bar{w}_8(\omega, q))$.

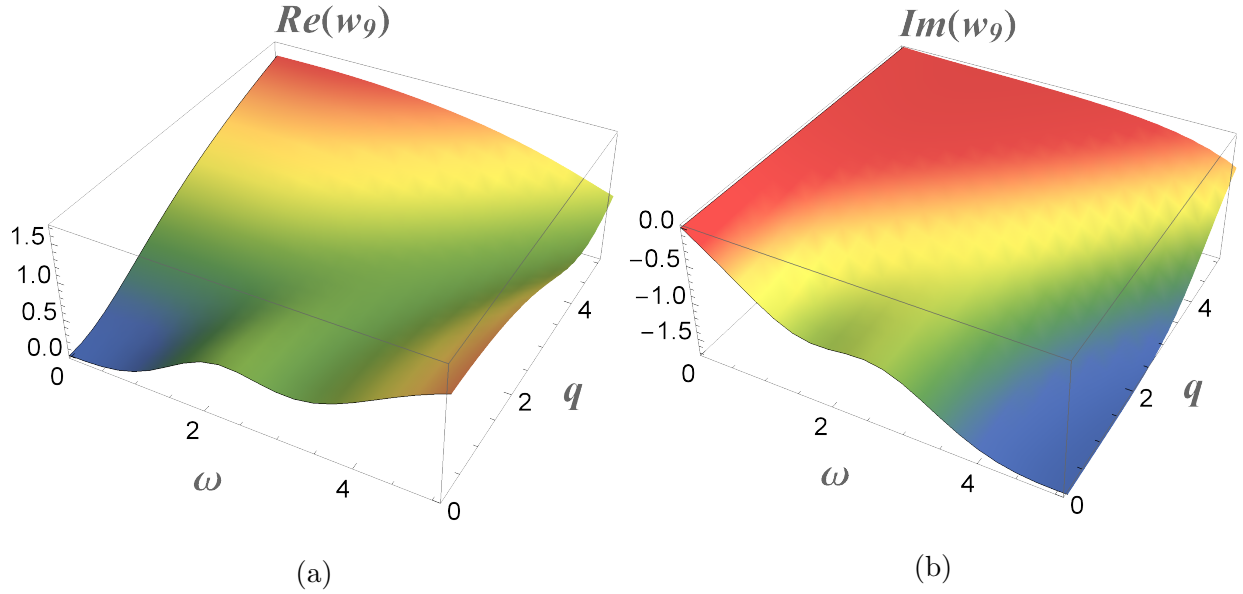


FIG. 11: Plots for ω -, q -dependence of the coefficients (a) $Re(w_9(\omega, q))$, (b) $Im(w_9(\omega, q))$.

- [2] D. Forster, *Hydrodynamic fluctuations, broken symmetry, and correlation functions*. CRC Press, 1975.
- [3] L. P. Kadanoff and P. C. Martin, “Hydrodynamic equations and correlation functions,” *Annals of Physics* **24** (Oct., 1963) 419–469.

- [4] M. Lublinsky and E. Shuryak, “Improved Hydrodynamics from the AdS/CFT,” *Phys. Rev. D* **80** (2009) 065026, [arXiv:0905.4069 \[hep-ph\]](#).
- [5] Y. Bu and M. Lublinsky, “Linearly resummed hydrodynamics in a weakly curved spacetime,” *JHEP* **04** (2015) 136, [arXiv:1502.08044 \[hep-th\]](#).
- [6] J. M. Maldacena, “The Large N limit of superconformal field theories and supergravity,” *Int. J. Theor. Phys.* **38** (1999) 1113–1133, [arXiv:hep-th/9711200](#).
- [7] S. Gubser, I. R. Klebanov, and A. M. Polyakov, “Gauge theory correlators from noncritical string theory,” *Phys. Lett. B* **428** (1998) 105–114, [arXiv:hep-th/9802109](#).
- [8] E. Witten, “Anti-de Sitter space and holography,” *Adv. Theor. Math. Phys.* **2** (1998) 253–291, [arXiv:hep-th/9802150](#).
- [9] P. Kovtun, D. T. Son, and A. O. Starinets, “Viscosity in strongly interacting quantum field theories from black hole physics,” *Phys. Rev. Lett.* **94** (2005) 111601, [arXiv:hep-th/0405231](#).
- [10] G. Policastro, D. T. Son, and A. O. Starinets, “The Shear viscosity of strongly coupled N=4 supersymmetric Yang-Mills plasma,” *Phys. Rev. Lett.* **87** (2001) 081601, [arXiv:hep-th/0104066](#).
- [11] G. Policastro, D. T. Son, and A. O. Starinets, “From AdS / CFT correspondence to hydrodynamics,” *JHEP* **09** (2002) 043, [arXiv:hep-th/0205052](#).
- [12] G. Policastro, D. T. Son, and A. O. Starinets, “From AdS / CFT correspondence to hydrodynamics. 2. Sound waves,” *JHEP* **12** (2002) 054, [arXiv:hep-th/0210220](#).
- [13] D. T. Son and A. O. Starinets, “Minkowski space correlators in AdS / CFT correspondence: Recipe and applications,” *JHEP* **09** (2002) 042, [arXiv:hep-th/0205051 \[hep-th\]](#).
- [14] S. Bhattacharyya, V. E. Hubeny, S. Minwalla, and M. Rangamani, “Nonlinear Fluid Dynamics from Gravity,” *JHEP* **02** (2008) 045, [arXiv:0712.2456 \[hep-th\]](#).
- [15] D. T. Son and A. O. Starinets, “Viscosity, Black Holes, and Quantum Field Theory,” *Ann. Rev. Nucl. Part. Sci.* **57** (2007) 95–118, [arXiv:0704.0240 \[hep-th\]](#).
- [16] Y. Bu and M. Lublinsky, “All order linearized hydrodynamics from fluid-gravity correspondence,” *Phys. Rev. D* **90** no. 8, (2014) 086003, [arXiv:1406.7222 \[hep-th\]](#).
- [17] Y. Bu and M. Lublinsky, “Linearized fluid/gravity correspondence: from shear viscosity to all order hydrodynamics,” *JHEP* **11** (2014) 064, [arXiv:1409.3095 \[hep-th\]](#).

- [18] Y. Bu, M. Lublinsky, and A. Sharon, “ $U(1)$ current from the AdS/CFT: diffusion, conductivity and causality,” *JHEP* **04** (2016) 136, [arXiv:1511.08789 \[hep-th\]](#).
- [19] S. Dubovsky, L. Hui, A. Nicolis, and D. T. Son, “Effective field theory for hydrodynamics: thermodynamics, and the derivative expansion,” *Phys. Rev.* **D85** (2012) 085029, [arXiv:1107.0731 \[hep-th\]](#).
- [20] S. Dubovsky, L. Hui, and A. Nicolis, “Effective field theory for hydrodynamics: Wess-Zumino term and anomalies in two spacetime dimensions,” *Phys. Rev.* **D89** no. 4, (2014) 045016, [arXiv:1107.0732 \[hep-th\]](#).
- [21] S. Endlich, A. Nicolis, R. A. Porto, and J. Wang, “Dissipation in the effective field theory for hydrodynamics: First order effects,” *Phys. Rev.* **D88** (2013) 105001, [arXiv:1211.6461 \[hep-th\]](#).
- [22] S. Grozdanov and J. Polonyi, “Viscosity and dissipative hydrodynamics from effective field theory,” *Phys. Rev. D* **91** no. 10, (2015) 105031, [arXiv:1305.3670 \[hep-th\]](#).
- [23] A. Nicolis, R. Penco, and R. A. Rosen, “Relativistic Fluids, Superfluids, Solids and Supersolids from a Coset Construction,” *Phys. Rev.* **D89** no. 4, (2014) 045002, [arXiv:1307.0517 \[hep-th\]](#).
- [24] P. Kovtun, G. D. Moore, and P. Romatschke, “Towards an effective action for relativistic dissipative hydrodynamics,” *JHEP* **07** (2014) 123, [arXiv:1405.3967 \[hep-ph\]](#).
- [25] M. Harder, P. Kovtun, and A. Ritz, “On thermal fluctuations and the generating functional in relativistic hydrodynamics,” *JHEP* **07** (2015) 025, [arXiv:1502.03076 \[hep-th\]](#).
- [26] F. M. Haehl, R. Loganayagam, and M. Rangamani, “The Fluid Manifesto: Emergent symmetries, hydrodynamics, and black holes,” *JHEP* **01** (2016) 184, [arXiv:1510.02494 \[hep-th\]](#).
- [27] F. M. Haehl, R. Loganayagam, and M. Rangamani, “Topological sigma models & dissipative hydrodynamics,” *JHEP* **04** (2016) 039, [arXiv:1511.07809 \[hep-th\]](#).
- [28] F. M. Haehl, R. Loganayagam, and M. Rangamani, “Effective Action for Relativistic Hydrodynamics: Fluctuations, Dissipation, and Entropy Inflow,” *JHEP* **10** (2018) 194, [arXiv:1803.11155 \[hep-th\]](#).
- [29] M. Crossley, P. Glorioso, and H. Liu, “Effective field theory of dissipative fluids,” *JHEP* **09** (2017) 095, [arXiv:1511.03646 \[hep-th\]](#).

- [30] P. Glorioso, M. Crossley, and H. Liu, “Effective field theory of dissipative fluids (II): classical limit, dynamical KMS symmetry and entropy current,” *JHEP* **09** (2017) 096, [arXiv:1701.07817 \[hep-th\]](#).
- [31] P. Glorioso and H. Liu, “The second law of thermodynamics from symmetry and unitarity,” [arXiv:1612.07705 \[hep-th\]](#).
- [32] P. Glorioso, H. Liu, and S. Rajagopal, “Global Anomalies, Discrete Symmetries, and Hydrodynamic Effective Actions,” *JHEP* **01** (2019) 043, [arXiv:1710.03768 \[hep-th\]](#).
- [33] K. Jensen, N. Pinzani-Fokeeva, and A. Yarom, “Dissipative hydrodynamics in superspace,” *JHEP* **09** (2018) 127, [arXiv:1701.07436 \[hep-th\]](#).
- [34] K. Jensen, R. Marjeh, N. Pinzani-Fokeeva, and A. Yarom, “A panoply of Schwinger-Keldysh transport,” *SciPost Phys.* **5** no. 5, (2018) 053, [arXiv:1804.04654 \[hep-th\]](#).
- [35] M. Crossley, P. Glorioso, H. Liu, and Y. Wang, “Off-shell hydrodynamics from holography,” *JHEP* **02** (2016) 124, [arXiv:1504.07611 \[hep-th\]](#).
- [36] J. de Boer, M. P. Heller, and N. Pinzani-Fokeeva, “Effective actions for relativistic fluids from holography,” *JHEP* **08** (2015) 086, [arXiv:1504.07616 \[hep-th\]](#).
- [37] P. Kovtun and L. G. Yaffe, “Hydrodynamic fluctuations, long time tails, and supersymmetry,” *Phys. Rev.* **D68** (2003) 025007, [arXiv:hep-th/0303010 \[hep-th\]](#).
- [38] P. Kovtun, G. D. Moore, and P. Romatschke, “The stickiness of sound: An absolute lower limit on viscosity and the breakdown of second order relativistic hydrodynamics,” *Phys. Rev.* **D84** (2011) 025006, [arXiv:1104.1586 \[hep-ph\]](#).
- [39] C. Young, J. I. Kapusta, C. Gale, S. Jeon, and B. Schenke, “Thermally Fluctuating Second-Order Viscous Hydrodynamics and Heavy-Ion Collisions,” *Phys. Rev.* **C91** no. 4, (2015) 044901, [arXiv:1407.1077 \[nucl-th\]](#).
- [40] Y. Akamatsu, A. Mazeliauskas, and D. Teaney, “A kinetic regime of hydrodynamic fluctuations and long time tails for a Bjorken expansion,” *Phys. Rev.* **C95** no. 1, (2017) 014909, [arXiv:1606.07742 \[nucl-th\]](#).
- [41] X. Chen-Lin, L. V. Delacretaz, and S. A. Hartnoll, “Theory of diffusive fluctuations,” *Phys. Rev. Lett.* **122** no. 9, (2019) 091602, [arXiv:1811.12540 \[hep-th\]](#).
- [42] A. Jain and P. Kovtun, “Non-universality of hydrodynamics,” [arXiv:2009.01356 \[hep-th\]](#).
- [43] M. Bluhm *et al.*, “Dynamics of critical fluctuations: Theory — phenomenology — heavy-ion collisions,” *Nucl. Phys.* **A1003** (2020) 122016, [arXiv:2001.08831 \[nucl-th\]](#).

- [44] P. Kovtun, “Lectures on hydrodynamic fluctuations in relativistic theories,” *J. Phys.* **A45** (2012) 473001, [arXiv:1205.5040 \[hep-th\]](#).
- [45] M. A. Stephanov, “Non-Gaussian fluctuations near the QCD critical point,” *Phys. Rev. Lett.* **102** (2009) 032301, [arXiv:0809.3450 \[hep-ph\]](#).
- [46] J. I. Kapusta and C. Young, “Causal Baryon Diffusion and Colored Noise,” *Phys. Rev.* **C90** no. 4, (2014) 044902, [arXiv:1404.4894 \[nucl-th\]](#).
- [47] K.-c. Chou, Z.-b. Su, B.-l. Hao, and L. Yu, “Equilibrium and Nonequilibrium Formalisms Made Unified,” *Phys. Rept.* **118** (1985) 1–131.
- [48] A. Kamenev, *Field Theory of Non-Equilibrium Systems*. Cambridge University Press, 2011.
- [49] E. A. Calzetta and B.-L. B. Hu, *Nonequilibrium Quantum Field Theory*. Cambridge University Press, 2009.
- [50] C. Herzog and D. Son, “Schwinger-Keldysh propagators from AdS/CFT correspondence,” *JHEP* **03** (2003) 046, [arXiv:hep-th/0212072](#).
- [51] K. Skenderis and B. C. van Rees, “Real-time gauge/gravity duality: Prescription, Renormalization and Examples,” *JHEP* **05** (2009) 085, [arXiv:0812.2909 \[hep-th\]](#).
- [52] K. Skenderis and B. C. van Rees, “Real-time gauge/gravity duality,” *Phys. Rev. Lett.* **101** (2008) 081601, [arXiv:0805.0150 \[hep-th\]](#).
- [53] E. Barnes, D. Vaman, C. Wu, and P. Arnold, “Real-time finite-temperature correlators from AdS/CFT,” *Phys. Rev.* **D82** (2010) 025019, [arXiv:1004.1179 \[hep-th\]](#).
- [54] D. Nickel and D. T. Son, “Deconstructing holographic liquids,” *New J. Phys.* **13** (2011) 075010, [arXiv:1009.3094 \[hep-th\]](#).
- [55] D. T. Son and D. Teaney, “Thermal Noise and Stochastic Strings in AdS/CFT,” *JHEP* **07** (2009) 021, [arXiv:0901.2338 \[hep-th\]](#).
- [56] J. de Boer, V. E. Hubeny, M. Rangamani, and M. Shigemori, “Brownian motion in AdS/CFT,” *JHEP* **07** (2009) 094, [arXiv:0812.5112 \[hep-th\]](#).
- [57] J. Sonner and A. G. Green, “Hawking Radiation and Non-equilibrium Quantum Critical Current Noise,” *Phys. Rev. Lett.* **109** (2012) 091601, [arXiv:1203.4908 \[cond-mat.str-el\]](#).
- [58] J. de Boer, M. P. Heller, and N. Pinzani-Fokeeva, “Holographic Schwinger-Keldysh effective field theories,” *JHEP* **05** (2019) 188, [arXiv:1812.06093 \[hep-th\]](#).

- [59] P. Glorioso, M. Crossley, and H. Liu, “A prescription for holographic Schwinger-Keldysh contour in non-equilibrium systems,” [arXiv:1812.08785 \[hep-th\]](#).
- [60] S. Caron-Huot, P. M. Chesler, and D. Teaney, “Fluctuation, dissipation, and thermalization in non-equilibrium AdS₅ black hole geometries,” *Phys. Rev. D* **84** (2011) 026012, [arXiv:1102.1073 \[hep-th\]](#).
- [61] P. M. Chesler and D. Teaney, “Dynamical Hawking Radiation and Holographic Thermalization,” [arXiv:1112.6196 \[hep-th\]](#).
- [62] M. Botta-Cantcheff, P. J. Martinez, and G. A. Silva, “The Gravity Dual of Real-Time CFT at Finite Temperature,” *JHEP* **11** (2018) 129, [arXiv:1808.10306 \[hep-th\]](#).
- [63] B. C. van Rees, “Real-time gauge/gravity duality and ingoing boundary conditions,” *Nucl. Phys. B Proc. Suppl.* **192-193** (2009) 193–196, [arXiv:0902.4010 \[hep-th\]](#).
- [64] B. Chakrabarty, J. Chakravarty, S. Chaudhuri, C. Jana, R. Loganayagam, and A. Sivakumar, “Nonlinear Langevin dynamics via holography,” *JHEP* **01** (2020) 165, [arXiv:1906.07762 \[hep-th\]](#).
- [65] C. Jana, R. Loganayagam, and M. Rangamani, “Open quantum systems and Schwinger-Keldysh holograms,” *JHEP* **07** (2020) 242, [arXiv:2004.02888 \[hep-th\]](#).
- [66] R. Loganayagam, K. Ray, and A. Sivakumar, “Fermionic Open EFT from Holography,” [arXiv:2011.07039 \[hep-th\]](#).
- [67] R. Loganayagam, K. Ray, S. K. Sharma, and A. Sivakumar, “Holographic KMS relations at finite density,” [arXiv:2011.08173 \[hep-th\]](#).
- [68] B. Chakrabarty and P. Aswin, “Open effective theory of scalar field in rotating plasma,” [arXiv:2011.13223 \[hep-th\]](#).
- [69] J. K. Ghosh, R. Loganayagam, S. G. Prabhu, M. Rangamani, A. Sivakumar, and V. Vishal, “Effective field theory of stochastic diffusion from gravity,” [arXiv:2012.03999 \[hep-th\]](#).
- [70] J. M. Maldacena, “Eternal black holes in anti-de Sitter,” *JHEP* **04** (2003) 021, [arXiv:hep-th/0106112](#).
- [71] G. T. Horowitz and M. M. Roberts, “Holographic Superconductors with Various Condensates,” *Phys. Rev. D* **78** (2008) 126008, [arXiv:0810.1077 \[hep-th\]](#).
- [72] R. C. Myers, A. O. Starinets, and R. M. Thomson, “Holographic spectral functions and diffusion constants for fundamental matter,” *JHEP* **11** (2007) 091, [arXiv:0706.0162 \[hep-th\]](#).

- [73] S. Caron-Huot, P. Kovtun, G. D. Moore, A. Starinets, and L. G. Yaffe, “Photon and dilepton production in supersymmetric Yang-Mills plasma,” *JHEP* **12** (2006) 015, [arXiv:hep-th/0607237](#).
- [74] F. M. Haehl, R. Loganayagam, and M. Rangamani, “Effective actions for anomalous hydrodynamics,” *JHEP* **03** (2014) 034, [arXiv:1312.0610 \[hep-th\]](#).
- [75] I. Iatrakis, S. Lin, and Y. Yin, “The anomalous transport of axial charge: topological vs non-topological fluctuations,” *JHEP* **09** (2015) 030, [arXiv:1506.01384 \[hep-th\]](#).
- [76] S. Lin, L. Yan, and G.-R. Liang, “Axial Charge Fluctuation and Chiral Magnetic Effect from Stochastic Hydrodynamics,” *Phys. Rev. C* **98** no. 1, (2018) 014903, [arXiv:1802.04941 \[nucl-th\]](#).